

May, 2002

Charmless Exclusive Baryonic B Decays

Hai-Yang Cheng^{1,2} and Kwei-Chou Yang³

¹ Institute of Physics, Academia Sinica
Taipei, Taiwan 115, Republic of China

² C.N. Yang Institute for Theoretical Physics, State University of New York
Stony Brook, New York 11794

³ Department of Physics, Chung Yuan Christian University
Chung-Li, Taiwan 320, Republic of China

Abstract

We present a systematical study of two-body and three-body charmless baryonic B decays. Branching ratios for two-body modes are in general very small, typically less than 10^{-6} , except that $\mathcal{B}(B^- \rightarrow p\bar{\Delta}^{--}) \sim 1 \times 10^{-6}$. In general, $\overline{B} \rightarrow N\bar{\Delta} > \overline{B} \rightarrow N\bar{N}$ due to the large coupling constant for $\Sigma_b \rightarrow B\Delta$. For three-body modes we focus on octet baryon final states. The leading three-dominated modes are $\overline{B}^0 \rightarrow p\bar{n}\pi^-(\rho^-)$, $n\bar{p}\pi^+(\rho^+)$ with a branching ratio of order 3×10^{-6} for $\overline{B}^0 \rightarrow p\bar{n}\pi^-$ and 8×10^{-6} for $\overline{B}^0 \rightarrow p\bar{n}\rho^-$. The penguin-dominated decays with strangeness in the meson, e.g., $B^- \rightarrow p\bar{p}K^{-(*)}$ and $\overline{B}^0 \rightarrow p\bar{n}K^{-(*)}$, $n\bar{n}\bar{K}^{0(*)}$, have appreciable rates and the $N\bar{N}$ mass spectrum peaks at low mass. The penguin-dominated modes containing a strange baryon, e.g., $\overline{B}^0 \rightarrow \Sigma^0\bar{p}\pi^+$, $\Sigma^-\bar{n}\pi^+$, have branching ratios of order $(1 \sim 4) \times 10^{-6}$. In contrast, the decay rate of $\overline{B}^0 \rightarrow \Lambda\bar{p}\pi^+$ is smaller. We explain why some of charmless three-body final states in which baryon-antibaryon pair production is accompanied by a meson have a larger rate than their two-body counterparts: either the pole diagrams for the former have an anti-triplet bottom baryon intermediate state, which has a large coupling to the B meson and the nucleon, or they are dominated by the factorizable external W -emission process.

I. INTRODUCTION

Inspired by the claim of the observation of the decay modes $p\bar{p}\pi^\pm$ and $p\bar{p}\pi^+\pi^-$ in B decays by ARGUS [1] in the late 1980s, baryonic B decays were studied extensively around the early 1990s [2–13] with the focus on the tree-dominated two-body decay modes, e.g. the charmful decays $B \rightarrow \Lambda_c \bar{N}$, $\Sigma_c \bar{N}$, and charmless ones $B \rightarrow p\bar{p}$, $\Lambda\bar{\Lambda}$. Up to now, none of the two-body baryonic B decays have been observed [14,15]. Many of the earlier model predictions are too large compared to experiment. For example, the previous limit on $\bar{B}^0 \rightarrow p\bar{p} < 7 \times 10^{-6}$ set by CLEO [14] has been recently pushed down to the level of 1.6×10^{-6} by Belle [15], whereas the model predictions are either too large or marginally comparable to the experimental limit (see Table II below).

The penguin-induced charmless baryonic B decays such as $\bar{B} \rightarrow \Sigma\bar{p}$, $\Sigma\bar{\Delta}$ have been studied by Chernyak and Zhitnitsky [7] based on the QCD sum rule analysis. They obtained the branching ratios of order $(0.3 - 1.0) \times 10^{-5}$. Experimentally, only the upper limits on $B^- \rightarrow \Lambda\bar{p}$, $\Lambda\bar{p}\pi^+\pi^-$, $\Delta^0\bar{p}$, $p\bar{\Delta}^{--}$ ($\bar{\Delta}^{--}$ being the antiparticle of Δ^{++}) and $\bar{B}^0 \rightarrow \Lambda\bar{p}\pi^+$ have been set.

As pointed out by Dunietz [16] and by Hou and Soni [17], the smallness of the two-body baryonic decay $B \rightarrow \mathcal{B}_1\bar{\mathcal{B}}_2$ has to do with a straightforward Dalitz plot analysis (see Sec. IV for a detailed discussion) or with the large energy release. Hou and Soni conjectured that in order to have larger baryonic B decays, one has to reduce the energy release and at the same time allow for baryonic ingredients to be present in the final state. Under this argument, the three-body decay, for example $B \rightarrow \rho p\bar{n}$, will dominate over the two-body mode $B \rightarrow p\bar{n}$ since the ejected ρ meson in the former decay carries away much energies and the configuration is more favorable for baryon production because of reduced energy release compared to the latter [18]. This is in contrast to the mesonic B decays where the two-body decay rate is generally comparable to the three-body one. The large rate of $B^0 \rightarrow D^{*-}p\bar{n}$ and $B^0 \rightarrow D^{*-}p\bar{p}\pi^+$ observed by CLEO [19] indicates that the decays $B \rightarrow$ baryons receive comparable contributions from $\bar{B} \rightarrow \Lambda_c\bar{p}X$ and $\bar{B} \rightarrow D\bar{N}\bar{N}'X$, as originally advocated by Dunietz [16]. A theoretical study of the decay $B \rightarrow D^*p\bar{n}$ has been carried out recently by [20]. In [21] we have shown explicitly that the three-body charmful decay $B^- \rightarrow \Lambda_c\bar{p}\pi^-(\rho^-)$ has indeed a magnitude larger than $\bar{B}^0 \rightarrow \Lambda_c\bar{p}$ as seen experimentally [22]. By the same token, it is expected that for charmless baryonic B decays, $\bar{B} \rightarrow (\pi, \rho)\mathcal{B}_1\bar{\mathcal{B}}_2$ are the dominant modes induced by tree operators and $\bar{B} \rightarrow (\pi, \rho)\mathcal{B}_{1(s)}\bar{\mathcal{B}}_2$, $\bar{B} \rightarrow K^{(*)}\mathcal{B}_1\bar{\mathcal{B}}_2$ are the leading modes induced by penguin diagrams. The recent first observation of the penguin-dominated charmless baryonic decay $B^- \rightarrow p\bar{p}K^-$ by Belle [23] clearly indicates that it has a much larger rate than the two-body counterpart $\bar{B}^0 \rightarrow p\bar{p}$. Of course, this does not necessarily imply that the three-body final state $\mathcal{B}_1\bar{\mathcal{B}}_2M$ always has a branching ratio larger than the two-body one $\mathcal{B}_1\bar{\mathcal{B}}_2$. We shall examine under what circumstance that the above argument holds.

In the present paper we will give a systematical study of two-body and three-body charm-

less baryonic B decays. The factorizable W -exchange or W -annihilation contribution to two-body decay modes is very small and hence negligible. For nonfactorizable contributions to two-body final states, we will calculate the corresponding pole diagrams at the hadron level. We will apply the bag model to evaluate the baryon-baryon matrix elements and find that the baryon-strange baryon weak transition is indeed dominated by penguin operators. Branching ratios for two-body baryonic modes are found to be in general very small $\lesssim \mathcal{O}(10^{-6})$ except for the decays with a Δ resonance in the final state.

The study of three-body baryonic decays is more complicated. Though it in general receives factorizable contributions, some of them involve three-body matrix elements and hence are not ready to evaluate. Therefore, pole diagrams still play an essential role. The baryonic decay with a vector meson in the final state normally has a large rate which should be easily accessible by the existing B factories.

The layout of the present paper is organized as follows. In Sec. II the issue of renormalization scheme and scale dependence of Wilson coefficients is addressed. We then study charmless two-body baryonic B decays in Sec. III and compare our results with the literature and experiment. In Sec. IV some important three-body modes are analyzed. Sec. V gives discussions and conclusions. A short summary of the relevant baryon wave functions and the bag model evaluation of baryon-baryon matrix elements are presented in the Appendix.

II. HAMILTONIAN

The relevant effective $\Delta B = 1$ weak Hamiltonian for hadronic charmless B decays is

$$\mathcal{H}_{\text{eff}}(\Delta B = 1) = \frac{G_F}{\sqrt{2}} \left\{ V_{ub} V_{uq}^* \left[c_1(\mu) O_1^u(\mu) + c_2(\mu) O_2^u(\mu) \right] + V_{cb} V_{cq}^* \left[c_1(\mu) O_1^c(\mu) + c_2(\mu) O_2^c(\mu) \right] \right. \\ \left. - V_{tb} V_{tq}^* \sum_{i=3}^{10} c_i(\mu) O_i(\mu) \right\} + \text{h.c.}, \quad (2.1)$$

where $q = d, s$, and

$$\begin{aligned} O_1^u &= (\bar{u}b)_{V-A} (\bar{q}u)_{V-A}, & O_2^u &= (\bar{u}_\alpha b_\beta)_{V-A} (\bar{q}_\beta u_\alpha)_{V-A}, \\ O_1^c &= (\bar{c}b)_{V-A} (\bar{q}c)_{V-A}, & O_2^c &= (\bar{c}_\alpha b_\beta)_{V-A} (\bar{q}_\beta c_\alpha)_{V-A}, \\ O_{3(5)} &= (\bar{q}b)_{V-A} \sum_{q'} (\bar{q}' q')_{V-A(V+A)}, & O_{4(6)} &= (\bar{q}_\alpha b_\beta)_{V-A} \sum_{q'} (\bar{q}'_\beta q'_\alpha)_{V-A(V+A)}, \\ O_{7(9)} &= \frac{3}{2} (\bar{q}b)_{V-A} \sum_{q'} e_{q'} (\bar{q}' q')_{V+A(V-A)}, & O_{8(10)} &= \frac{3}{2} (\bar{q}_\alpha b_\beta)_{V-A} \sum_{q'} e_{q'} (\bar{q}'_\beta q'_\alpha)_{V+A(V-A)}, \end{aligned} \quad (2.2)$$

with O_3 – O_6 being the QCD penguin operators, O_7 – O_{10} the electroweak penguin operators and $(\bar{q}_1 q_2)_{V\pm A} \equiv \bar{q}_1 \gamma_\mu (1 \pm \gamma_5) q_2$. The scale dependent Wilson coefficients calculated at next-to-leading order are renormalization scheme dependent. We use the next-to-leading Wilson coefficients evaluated in the naive dimensional regularization scheme [24]

$$c_1 = 1.082, \quad c_2 = -0.185, \quad c_3 = 0.014, \quad c_4 = -0.035, \quad c_5 = 0.009, \quad c_6 = -0.041, \\ c_7/\alpha = -0.002, \quad c_8/\alpha = 0.054, \quad c_9/\alpha = -1.292, \quad c_{10}/\alpha = 0.263, \quad c_g = -0.143, \quad (2.3)$$

at $\mu = \overline{m}_b(m_b) = 4.40$ GeV for $\Lambda_{\overline{\text{MS}}}^{(5)} = 225$ MeV taken from Table XXII of [24] with α being an electromagnetic fine-structure coupling constant. In order to ensure that the physical amplitude is renormalization scale and γ_5 -scheme independent, we include vertex and penguin corrections to hadronic matrix elements of four-quark operators [25,26]. This amounts to modifying $c_i(\mu) \rightarrow c_i^{\text{eff}}$ and

$$\sum c_i(\mu) \langle Q_i(\mu) \rangle = \sum c_i^{\text{eff}} \langle Q_i \rangle_{\text{VIA}}, \quad (2.4)$$

where the subscript VIA means that the hadronic matrix element is evaluated under the vacuum insertion approximation. Numerical results for c_i^{eff} are shown in Table I (for details, see [25]). It should be stressed that c_i^{eff} are renormalization scale and scheme independent. For the mesonic decay $B \rightarrow M_1 M_2$ with two mesons in the final state, two of the four quarks involving in the vertex diagrams will form an ejected meson. In this case, it is necessary to take into account the convolution with the ejected meson wave function.

The penguin matrix element of scalar and pseudoscalar densities, $\langle \mathcal{B}_1 \overline{\mathcal{B}}_2 | \bar{q}_1 (1 \pm \gamma_5) q_2 | 0 \rangle$, is usually evaluated by applying the equation of motion and it is renormalization scale and scheme dependent. Since the factorization scale is set at $\mu_f = m_b$ to obtain the effective Wilson coefficients listed in Table I, we will therefore evaluate the penguin matrix element of scalar and pseudoscalar densities at the m_b scale.

TABLE I. Numerical values of the effective Wilson coefficients c_i^{eff} for $b \rightarrow s$, $b \rightarrow d$ and $\bar{b} \rightarrow \bar{d}$ transitions evaluated at $\mu_f = m_b$ and $k^2 = m_b^2/2$ taken from Table I of [26], where use of $|V_{ub}/V_{cb}| = 0.085$ has been made. The numerical results are insensitive to the unitarity angle γ .

	$b \rightarrow s, \bar{b} \rightarrow \bar{s}$	$b \rightarrow d$	$\bar{b} \rightarrow \bar{d}$
c_1^{eff}	1.169	1.169	1.169
c_2^{eff}	-0.367	-0.367	-0.367
c_3^{eff}	$0.0227 + i0.0045$	$0.0226 + i0.0038$	$0.0230 + i0.0051$
c_4^{eff}	$-0.0463 - i0.0136$	$-0.0460 - i0.0114$	$-0.0470 - i0.0154$
c_5^{eff}	$0.0134 + i0.0045$	$0.0133 + i0.0038$	$0.0137 + i0.0051$
c_6^{eff}	$-0.0600 - i0.0136$	$-0.0597 - i0.0114$	$-0.0608 - i0.0154$
c_7^{eff}/α	$-0.0309 - i0.0367$	$-0.0305 - i0.0324$	$-0.0326 - i0.0403$
c_8^{eff}/α	0.070	0.070	0.070
c_9^{eff}/α	$-1.428 - i0.0367$	$-1.428 - i0.0324$	$-1.430 - i0.0403$
$c_{10}^{\text{eff}}/\alpha$	0.48	0.48	0.48

For quark mixing matrix elements, we will use $|V_{ub}/V_{cb}| = 0.085$ and the unitary angle $\gamma = 60^\circ$. In terms of the Wolfenstein parameters $A = 0.815$ and $\lambda = 0.2205$ we have

$$\rho = 0.385 \sin \gamma, \quad \eta = 0.385 \cos \gamma, \quad (2.5)$$

where ρ and η are the parameters in the Wolfenstein parametrization [27] of the quark mixing matrix.

III. CHARMLESS TWO-BODY BARYONIC DECAYS

The charmless B decays into two light baryons can be classified into two categories: the ones induced by the $b \rightarrow u$ tree transition, and the ones by the $b \rightarrow s$ penguin transition. The decay amplitude of $B \rightarrow \mathcal{B}_1(\frac{1}{2}^+) \bar{\mathcal{B}}_2(\frac{1}{2}^+)$ has the form

$$\mathcal{A}(B \rightarrow \mathcal{B}_1 \bar{\mathcal{B}}_2) = \bar{u}_1(A + B\gamma_5)v_2, \quad (3.1)$$

where A and B correspond to p -wave parity-violating (PV) and s -wave parity-conserving (PC) amplitudes, respectively. The decay rate is given by

$$\Gamma(B \rightarrow \mathcal{B}_1(1/2^+) \bar{\mathcal{B}}_2(1/2^+)) = \frac{p_c}{4\pi} \left\{ |A|^2 \frac{(m_B + m_1 + m_2)^2 p_c^2}{(E_1 + m_1)(E_2 + m_2)m_B^2} \right. \\ \left. + |B|^2 \frac{[(E_1 + m_1)(E_2 + m_2) + p_c^2]^2}{(E_1 + m_1)(E_2 + m_2)m_B^2} \right\}, \quad (3.2)$$

where p_c is the c.m. momentum, E_i and m_i are the energy and mass of the baryon \mathcal{B}_i , respectively. For the decay $B \rightarrow \mathcal{B}_1(\frac{3}{2}^+) \bar{\mathcal{B}}_2(\frac{1}{2}^+)$ with a spin- $\frac{3}{2}$ baryon in the final state, the general amplitude reads

$$\mathcal{A}(B \rightarrow \mathcal{B}_1(p_1) \bar{\mathcal{B}}_2(p_2)) = iq_\mu \bar{u}_1^\mu(p_1)(C + D\gamma_5)v_2(p_2), \quad (3.3)$$

where u^μ is the Rarita-Schwinger vector spinor for a spin- $\frac{3}{2}$ particle, $q = p_1 - p_2$ and C , D correspond to parity-violating p -wave and parity-conserving d -wave amplitudes, respectively. The corresponding decay rate is

$$\Gamma(B \rightarrow \mathcal{B}_1(3/2^+) \bar{\mathcal{B}}_2(1/2^+)) = \frac{p_c^3}{6\pi} \frac{1}{m_1^2} \left\{ |C|^2 \frac{[(E_1 + m_1)(E_2 + m_2) + p_c^2]^2}{(E_1 + m_1)(E_2 + m_2)m_B^2} \right. \\ \left. + |D|^2 \frac{(m_B + m_1 + m_2)^2 p_c^2}{(E_1 + m_1)(E_2 + m_2)m_B^2} \right\}. \quad (3.4)$$

As shown in Fig. 1, the quark diagrams for two-body baryonic B decays consist of internal W -emission diagram, $b \rightarrow d(s)$ penguin transition, W -exchange for the neutral B meson and W -annihilation for the charged B . Just as mesonic B decays, W -exchange and W -annihilation are expected to be helicity suppressed and the former is furthermore subject to color suppression.* In the language of the pole model, the $M^{(*)}\mathcal{B}_1 \bar{\mathcal{B}}_2$ form factor

*In contrast, W -exchange plays an essential role in nonleptonic decays of baryons as it is no longer subject to color and helicity suppression.

is expected to be largely suppressed at $q^2 = m_B^2$. As estimated by [5,10,13], the W -exchange or W -annihilation contribution is very insignificant and hence can be neglected. The tree-dominated decays, e.g. $\overline{B}^0 \rightarrow p\bar{p}$, $p\bar{\Delta}^-$ are mainly induced by the internal W -emission via $b \rightarrow u$ transition, while penguin-dominated modes, e.g. $B^- \rightarrow \Lambda\bar{p}$, $\Sigma^0\bar{p}$ proceed through $b \rightarrow s$ penguin transition. These amplitudes are nonfactorizable and thus very difficult to evaluate directly. This is the case in particular for baryons, which being made out of three quarks, in contrast to two quarks for mesons, bring along several essential complications. In order to circumvent this difficulty, it is customary to assume that the decay amplitude at the hadron level is dominated by the pole diagrams with low-lying one-particle intermediate states. More precisely, PC and PV amplitudes are dominated by $\frac{1}{2}^+$ ground-state intermediate states and $\frac{1}{2}^-$ low-lying baryon resonances, respectively [10].[†] This pole model has been applied successfully to nonleptonic decays of hyperons and charmed baryons [28,29]. In general, the pole diagram leads to

$$A = - \sum_{\mathcal{B}_b^*} \frac{g_{\mathcal{B}_b^* \rightarrow B\mathcal{B}_2} b_{\mathcal{B}_b^* \mathcal{B}_1}}{m_1 - m_{\mathcal{B}_b^*}}, \quad B = \sum_{\mathcal{B}_b} \frac{g_{\mathcal{B}_b \rightarrow B\mathcal{B}_2} a_{\mathcal{B}_b \mathcal{B}_1}}{m_1 - m_{\mathcal{B}_b}}, \quad (3.5)$$

where

$$\langle \mathcal{B}_1 | \mathcal{H}_{\text{eff}}^{\text{PC}} | \mathcal{B}_b \rangle = \bar{u}_{\mathcal{B}_1} a_{\mathcal{B}_b \mathcal{B}_1} u_{\mathcal{B}_b}, \quad \langle \mathcal{B}_1 | \mathcal{H}_{\text{eff}}^{\text{PV}} | \mathcal{B}_b^* \rangle = i \bar{u}_{\mathcal{B}_1} b_{\mathcal{B}_b^* \mathcal{B}_1} u_{\mathcal{B}_b^*} \quad (3.6)$$

are PC and PV matrix elements, respectively.

Since the weak transition does not involve momentum transfer, it can be evaluated using the quark model. Conventionally, baryon matrix elements are evaluated using the bag model or the harmonic oscillator model. In the present work we prefer to employ the MIT bag model [30] to compute the weak baryon-baryon transition for several reasons. First, it has been applied successfully to describe the p -wave amplitudes of hyperon nonleptonic decays and it is much simpler than the harmonic oscillator model for computing the PC matrix elements. Second, it is relatively easy to incorporate penguin operators in calculations. Third and most importantly, the bag model calculation gives predictions consistent with experiment, whereas the calculated results based on the harmonic-oscillator model are too large compared to the data. This will be clearly demonstrated below when we discuss $B \rightarrow p\bar{p}$ and $p\bar{\Delta}$.

However, it is known that the bag model is considerably less successful for describing the physical non-charm and non-bottom $\frac{1}{2}^-$ resonances [30], not mentioning the charm or bottom $\frac{1}{2}^-$ baryon states. Therefore, we will not evaluate the PV matrix element $b_{\mathcal{B}_b^* \mathcal{B}}$ and the strong coupling $g_{\mathcal{B}_b^* \rightarrow B\mathcal{B}_2}$ as their calculations in the bag model are much more involved and are far more uncertain than the PC case [28]. Fortunately, there are some decay modes that are purely parity-conserving within the framework of the 3P_0 quark-pair-creation model to be mentioned shortly. Examples are $B^- \rightarrow n\bar{p}$ and $\overline{B} \rightarrow N\bar{\Delta}$, which will be discussed below.

[†]The s -channel meson pole states correspond to weak annihilation diagrams [see Fig. 1(b)].

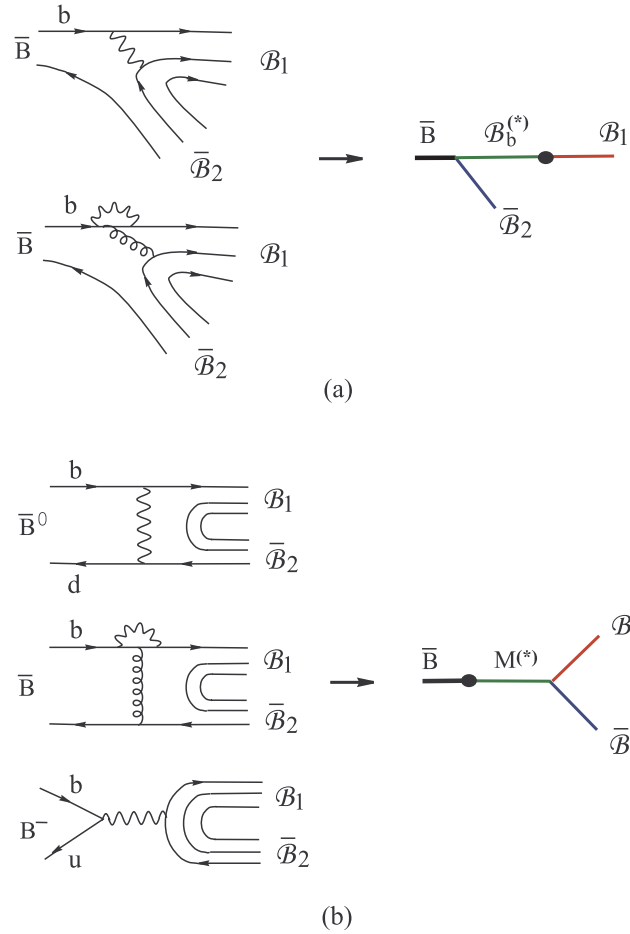


FIG. 1. Quark and pole diagrams for $\bar{B} \rightarrow \mathcal{B}_1 \bar{\mathcal{B}}_2$ where the symbol \bullet denotes the weak vertex. Fig. 1(a) corresponds to the nonfactorizable internal W emission or the $b \rightarrow d(s)$ penguin transition, while Fig. 1(b) to the W -exchange contribution for the neutral B or W -annihilation for the charged B , or penguin-induced weak annihilation.

For strong couplings we will follow [10,31] to adopt the 3P_0 quark-pair-creation model in which the $q\bar{q}$ pair is created from the vacuum with vacuum quantum numbers 3P_0 . We shall apply this model to estimate the relative strong coupling strength and choose $|g_{\Sigma_b^+ \rightarrow \bar{B}^0 p}| = 5$ as a benchmarked value for the absolute coupling strength (see below). Presumably, the 3P_0 model works in the nonperturbative low energy regime. In contrast, in the perturbative high energy region where perturbative QCD is applicable, it is expected that the quark pair is created perturbatively via one gluon exchange with one-gluon quantum numbers 3S_1 . Since the light baryons produced in two-body baryonic B decays are very energetic, it appears that the 3S_1 model may be more relevant. However, in the present paper we adopt the 3P_0 model for quark pair creation for the following two reasons. First, it is much simpler to estimate the relative strong coupling strength in the 3P_0 model rather than in the 3S_1 model where hard gluons arise from four different quark legs and generally involve infrared problems. Second, this model is presumably reliable for estimating the $\mathcal{B}_b \mathcal{B}B$ coupling when all particles are on their mass shell. Of course, the intermediate pole state \mathcal{B}_b in the two-body baryonic decay is far from its mass shell (but not quite so in the three-body decay). In principle, one can treat the intermediate state as an on-shell particle and then assume that off-shell effects of the pole can be parametrized in terms of form factors. Such form factors are basically unknown, though they are expected to become smaller as the intermediate state is more away from its mass shell due to less overlap of initial and final hadron wave functions. Since we are interested in the relative strength of strong couplings rather than the absolute strength, it seems plausible to assume that the relative coupling strengths are essentially not affected by the off-shell extrapolation; that is, the strong form factors are assumed to be universal. We then use the experimental result for $B^- \rightarrow \Lambda_c \bar{p} \pi^-$ to fix the absolute coupling strength of $g_{\Lambda_b^+ \rightarrow \bar{B}^0 p}$ or $g_{\Sigma_b^+ \rightarrow \bar{B}^0 p}$ [21].[‡] In the future, it is important to carry out the more sophisticated pQCD analysis to gain a better understanding of the underlying decay mechanism for baryonic B decays.

At this point, we would like to stress that although we employ the same pole-model framework as Jarfi *et al.* [10] to discuss baryonic B decays, the calculational detail is different. While Jarfi *et al.* evaluated baryon matrix elements at large momentum transfer and strong couplings at small transfer, we consider weak transition at zero transfer and strong couplings at large momentum transfer as elaborated before. Another difference is related to the quark model evaluation of baryon matrix elements: We employ the bag model rather than the harmonic oscillator model.

[‡]The nonresonant decay $B^- \rightarrow \Lambda_c \bar{p} \pi^-$ receives main contributions from Figs. 2(a) and 2(d) shown in Sec. IV (see [21]). In the pole model, the contribution of the former is governed by the Λ_b pole. Therefore, a measurement of the decay rate of this mode enables us to determine the off-shell coupling $g_{\Lambda_b^+ \rightarrow \bar{B}^0 p}$. For detail, see [21].

TABLE II. Predictions of the branching ratios for some charmless two-body baryonic B decays classified into two categories: tree-dominated and penguin-dominated. In this work, some branching ratios denoted by “†” are calculated only for the parity-conserving part. For comparison some other predictions in the literature are also shown. We have normalized the branching ratios to $|V_{ub}/V_{cb}| = 0.085$. The predictions given in [11] are carried out in two different quark-pair-creation models: local and nonlocal. The line separates tree- and penguin-dominated charmless baryonic B decays and experimental limits are taken from [14,15].

	Ref. [3]	Ref. [7]	Ref. [10]	Ref.[11]		This work	Expt.
				non-local	local		
$\overline{B}^0 \rightarrow p\bar{p}$	4.2×10^{-6}	1.2×10^{-6}	7.0×10^{-6}	2.9×10^{-6}	2.7×10^{-5}	$1.1 \times 10^{-7}\dagger$	$< 1.2 \times 10^{-6}$
$\overline{B}^0 \rightarrow n\bar{n}$			3.5×10^{-7}	7.0×10^{-6}	2.9×10^{-6}	2.7×10^{-5}	$1.2 \times 10^{-7}\dagger$
$B^- \rightarrow n\bar{p}$			6.9×10^{-7}	1.7×10^{-5}	0	0	5.0×10^{-7}
$\overline{B}^0 \rightarrow \Lambda\bar{\Lambda}$				2×10^{-7}		$0\dagger$	$< 1.0 \times 10^{-6}$
$B^- \rightarrow p\bar{\Delta}^{--}$	1.5×10^{-4}	2.9×10^{-7}	3.2×10^{-4}	2.4×10^{-6}	8.7×10^{-6}	1.4×10^{-6}	$< 1.5 \times 10^{-4}$
$\overline{B}^0 \rightarrow p\bar{\Delta}^-$			7×10^{-8}	1.0×10^{-4}	1.0×10^{-6}	4.0×10^{-6}	4.3×10^{-7}
$B^- \rightarrow n\bar{\Delta}^-$				1.1×10^{-4}	2.7×10^{-7}	1×10^{-7}	4.6×10^{-7}
$\overline{B}^0 \rightarrow n\bar{\Delta}^0$				1.0×10^{-4}	1.0×10^{-6}	4.0×10^{-6}	4.3×10^{-7}
$B^- \rightarrow \Lambda\bar{p}$			$\lesssim 3 \times 10^{-6}$			$2.2 \times 10^{-7}\dagger$	$< 2.2 \times 10^{-6}$
$\overline{B}^0 \rightarrow \Lambda\bar{n}$						$2.1 \times 10^{-7}\dagger$	
$\overline{B}^0 \rightarrow \Sigma^+\bar{p}$			6×10^{-6}			$1.8 \times 10^{-8}\dagger$	
$B^- \rightarrow \Sigma^0\bar{p}$			3×10^{-6}			$5.8 \times 10^{-8}\dagger$	
$B^- \rightarrow \Sigma^+\bar{\Delta}^{--}$			6×10^{-6}			2.0×10^{-7}	
$\overline{B}^0 \rightarrow \Sigma^+\bar{\Delta}^-$			6×10^{-6}			6.3×10^{-8}	
$B^- \rightarrow \Sigma^-\bar{\Delta}^0$			2×10^{-6}			8.7×10^{-8}	

For the reader’s convenience, in Table II we give a summary of the calculational results presented in Sections III.A and III.B below. For comparison, some other predictions in the literature are shown in the same table.

A. Tree-dominated two-body decays

1. $\overline{B}^0 \rightarrow p\bar{p}$

As discussed before, we can neglect W -exchange contributions to $\overline{B}^0 \rightarrow p\bar{p}$ and simply focus on the internal W -emission which is manifested as the pole diagram at the hadron level with the low-lying intermediate states $\Sigma_b^{+(*)}$ [see Fig.1(a)]. The PV and PC wave amplitudes read

$$A = -\frac{g_{\Sigma_b^{*+} \rightarrow \bar{B}^0 p} b_{\Sigma_b^{*+} p}}{m_p - m_{\Sigma_b^*}}, \quad B = \frac{g_{\Sigma_b^+ \rightarrow \bar{B}^0 p} a_{\Sigma_b^+ p}}{m_p - m_{\Sigma_b}}. \quad (3.7)$$

Neglecting penguin contributions to the matrix element due to the smallness of penguin coefficients, we have

$$a_{\Sigma_b^+ p} = \frac{G_F}{\sqrt{2}} V_{ub} V_{ud}^* (c_1^{\text{eff}} - c_2^{\text{eff}}) \langle p | O_1^{\text{PC}} | \Sigma_b^+ \rangle \quad (3.8)$$

for the PC matrix element, where $O_1 = (\bar{u}b)_{V-A} (\bar{d}u)_{V-A}$ and use has been made of $\langle p | O_2 | \Sigma_b^+ \rangle = -\langle p | O_1 | \Sigma_b^+ \rangle$. The latter relation holds because the combination of the four-quark operators $O_1 + O_2$ is symmetric in color indices (more precisely, it is a color sextet) and hence it does not contribute to the baryon-baryon matrix element since the baryon-color wave function is totally antisymmetric. In contrast, the operator $O_1 - O_2$ is a color antitriplet and has isospin $I = \frac{1}{2}$ because the diquark ud is isoscalar due to anti-symmetrization. The latter feature will lead to some $\Delta I = \frac{1}{2}$ rule relations, for example (3.26) below.

We shall employ the MIT bag model [30] to evaluate the baryon matrix elements (see e.g. [28,29] for the method). From the Appendix of [21] or [28] we obtain the PC matrix element

$$\langle p | O_1^{\text{PC}} | \Sigma_b^+ \rangle = -6X(4\pi), \quad (3.9)$$

where

$$X = \int_0^R r^2 dr [u_u(r)u_b(r) + v_u(r)v_b(r)][u_d(r)u_u(r) + v_d(r)v_u(r)], \quad (3.10)$$

is a four-quark overlap bag integral and $u_q(r)$, $v_q(r)$ are the large and small components of the quark wave functions in the ground ($1S_{1/2}$) state (see, for example, [21]). As stressed in passing, we will not evaluate the PV matrix element $b_{\Sigma_b^* p}$ as its calculation in the bag model is much more involved and considerably less reliable than the PC one. (However, see [28,29] for the evaluation of PV matrix elements in charmed baryon decays.) Numerically, we obtain

$$X = 1.52 \times 10^{-4} \text{ GeV}^3. \quad (3.11)$$

Collecting everything together leads to

$$\mathcal{B}(\bar{B}^0 \rightarrow p\bar{p})_{\text{PC}} = 1.1 \times 10^{-7} \left| \frac{g_{\Sigma_b^+ \rightarrow \bar{B}^0 p}}{5} \right|^2, \quad (3.12)$$

and hence

$$\mathcal{B}(\bar{B}^0 \rightarrow p\bar{p}) \lesssim 2.2 \times 10^{-7} \left| \frac{g_{\Sigma_b^+ \rightarrow \bar{B}^0 p}}{5} \right|^2, \quad (3.13)$$

where the upper limit corresponds to $\Gamma_{\text{PV}}/\Gamma_{\text{PC}} = 1$. Therefore, the above result is consistent with the experimental limit 1.6×10^{-6} [15].

We have chosen $|g_{\Sigma_b^+ \rightarrow \bar{B}^0 p}| = 5$ as a benchmarked value for the strong coupling for two reasons. First, a calculation based on the 3P_0 quark-pair-creation model yields a value of $6 \sim 10$ for this coupling [10]. Second, we have computed the decay $B^- \rightarrow \Lambda_c \bar{p} \pi^-$ in [21]. A fit to the measured branching ratio for this mode implies a strong coupling $g_{\Lambda_b \rightarrow B^- p}$ with the strength in the vicinity of order 16. Using the relation $|g_{\Lambda_b \rightarrow B^- p}| = 3\sqrt{3/2} |g_{\Sigma_b^+ \rightarrow \bar{B}^0 p}|$ derived from the 3P_0 quark-pair-creation model, it follows that $|g_{\Sigma_b^+ \rightarrow \bar{B}^0 p}| \sim 4.4$, which is close to the above-mentioned model estimate.

Note that a similar pole model calculation by Jarfi *et al.* [10] yields a branching ratio of order 7.0×10^{-5} after scaling their original result (see Table I of [10]) to $|V_{ub}/V_{cb}| = 0.085$ and to the current world average of B lifetimes [32]. Since $\Gamma_{\text{PV}}/\Gamma_{\text{PC}} = 0.79$ is obtained by the same authors, and a strong coupling $|g_{\Sigma_b^+ \rightarrow \bar{B}^0 p}| = 10$ is used by them, it follows that

$$\mathcal{B}(\bar{B}^0 \rightarrow p\bar{p})_{\text{PC}}^{\text{H.O.}} = 1.0 \times 10^{-6} \left| \frac{g_{\Sigma_b^+ \rightarrow \bar{B}^0 p}}{5} \right|^2 \quad (3.14)$$

is predicted by Jarfi *et al.* [10] using the harmonic oscillator wave functions for baryons. Evidently, the estimate of the PC matrix element $a_{\Sigma_b^+ p}$ in the harmonic oscillator model is about three times as big as the one calculated in the bag model.[§]

2. $\bar{B}^0 \rightarrow n \bar{n}$, $B^- \rightarrow n\bar{p}$

The relevant intermediate states in the pole diagrams for the decays $\bar{B}^0 \rightarrow n \bar{n}$ and $B^- \rightarrow n\bar{p}$ are $\Lambda_b^{(*)}$ and $\Sigma_b^{0(*)}$. Consider the former decay first. The PV and PC wave amplitudes read

$$A = -\frac{g_{\Sigma_b^{0*} \rightarrow \bar{B}^0 n} b_{\Sigma_b^{0*} n}}{m_n - m_{\Sigma_b^*}} - \frac{g_{\Lambda_b^* \rightarrow \bar{B}^0 n} b_{\Lambda_b^* n}}{m_n - m_{\Lambda_b^*}}, \quad B = \frac{g_{\Sigma_b^0 \rightarrow \bar{B}^0 n} a_{\Sigma_b^0 n}}{m_n - m_{\Sigma_b}} + \frac{g_{\Lambda_b \rightarrow \bar{B}^0 n} a_{\Lambda_b n}}{m_n - m_{\Lambda_b}}. \quad (3.15)$$

Applying the bag model leads to the PC matrix elements

$$\langle n | O_1^{\text{PC}} | \Sigma_b^0 \rangle = 3\sqrt{2}X(4\pi), \quad \langle n | O_1^{\text{PC}} | \Lambda_b \rangle = \sqrt{6}X(4\pi). \quad (3.16)$$

For strong couplings, the 3P_0 quark-pair-creation model implies [31]

$$\frac{g_{\Lambda_b \rightarrow \bar{B}^0 n}}{g_{\Sigma_b^0 \rightarrow \bar{B}^0 n}} = \frac{\langle \Phi_{n\uparrow}(124) \Phi_{\bar{B}^0}(35) | \Phi_{\Lambda_b^{\uparrow}}(123) \Phi_{\text{vac}}(45) \rangle}{\langle \Phi_{n\uparrow}(124) \Phi_{\bar{B}^0}(35) | \Phi_{\Sigma_b^{0\uparrow}}(123) \Phi_{\text{vac}}(45) \rangle}, \quad (3.17)$$

[§]It is not clear to us how to make a direct comparison of our result for $a_{\Sigma_b^+ p}$, which has a dimension of mass, with the numerical value of $a_{\Sigma_b^+ p}$ shown in Table II of [10] which seems to be dimensionless.

where the Φ 's are the spin-flavor wave functions and the vacuum wave function has the expression

$$\Phi_{\text{vac}} = \frac{1}{\sqrt{3}}(u\bar{u} + d\bar{d} + s\bar{s}) \otimes \frac{1}{\sqrt{2}}(\uparrow\downarrow + \downarrow\uparrow). \quad (3.18)$$

Using the baryon wave functions given in Eq. (A1) and the B meson wave function

$$\Phi_{\overline{B}^0} = b\bar{d} \otimes \frac{1}{\sqrt{2}}(\uparrow\downarrow - \downarrow\uparrow), \quad (3.19)$$

we obtain

$$g_{\Lambda_b \rightarrow \overline{B}^0 n} = -3\sqrt{3} g_{\Sigma_b^0 \rightarrow \overline{B}^0 n}. \quad (3.20)$$

Consequently,

$$B(\overline{B}^0 \rightarrow n\bar{n}) = -g_{\Sigma_b^0 \rightarrow \overline{B}^0 n} \left(\frac{3\sqrt{3} a_{\Lambda_b n}}{m_n - m_{\Lambda_b}} - \frac{a_{\Sigma_b^0 n}}{m_n - m_{\Sigma_b}} \right). \quad (3.21)$$

Likewise, for $B^- \rightarrow n\bar{p}$ we have

$$B(B^- \rightarrow n\bar{p}) = g_{\Sigma_b^0 \rightarrow \overline{B}^0 n} \left(\frac{3\sqrt{3} a_{\Lambda_b n}}{m_p - m_{\Lambda_b}} + \frac{a_{\Sigma_b^0 n}}{m_p - m_{\Sigma_b}} \right), \quad (3.22)$$

where use has been made of

$$g_{\Lambda_b \rightarrow B^- p} = 3\sqrt{3} g_{\Sigma_b^0 \rightarrow \overline{B}^0 n}, \quad g_{\Sigma_b^0 \rightarrow B^- p} = g_{\Sigma_b^0 \rightarrow \overline{B}^0 n}. \quad (3.23)$$

Using the relations

$$g_{\Sigma_b^0 \rightarrow \overline{B}^0 n} = -\frac{1}{\sqrt{2}} g_{\Sigma_b^+ \rightarrow \overline{B}^0 p}, \quad (3.24)$$

and

$$a_{\Sigma_b^0 n} = -\frac{1}{\sqrt{2}} a_{\Sigma_b^+ p} \quad (3.25)$$

derived from Eqs. (3.9) and (3.16), we find that $\overline{B} \rightarrow N\overline{N}$ amplitudes satisfy the $\Delta I = 1/2$ relation [5,10]

$$\mathcal{A}(\overline{B}^0 \rightarrow p\bar{p}) - \mathcal{A}(\overline{B}^0 \rightarrow n\bar{n}) = \mathcal{A}(B^- \rightarrow n\bar{p}). \quad (3.26)$$

As mentioned before, this $\Delta I = \frac{1}{2}$ relation arises because the weak operator $O_1 - O_2$ has isospin $I = \frac{1}{2}$.

From Eqs. (3.16), (3.21) and (3.22), it is evident that $B^- \rightarrow n\bar{p}$ has a larger rate than $\overline{B}^0 \rightarrow n\bar{n}$. In contrast, the QCD sum rule analysis in [7] predicts that $\Gamma(\overline{B}^0 \rightarrow p\bar{p}) > \Gamma(B^- \rightarrow n\bar{p}) > \Gamma(\overline{B}^0 \rightarrow n\bar{n})$. Moreover, as pointed out in [5,10], the decay $B^- \rightarrow n\bar{p}$ is

purely parity-conserving, namely, its parity-violating amplitude vanishes provided that the $q\bar{q}$ pair is created from the vacuum. As pointed out by Körner [5], if the quark pair is created perturbatively via one gluon exchange with one-gluon quantum number (3S_1 model), the neutron in $B^- \rightarrow n\bar{p}$ will have a positive longitudinal polarization. Therefore, a polarization measurement of the neutron by studying its subsequent weak decay can be used to test the 3P_0 and 3S_1 quark-pair-creation models.

We are ready to compute branching ratios and obtain

$$\begin{aligned}\mathcal{B}(\overline{B}^0 \rightarrow n\bar{n})_{\text{PC}} &= 1.2 \times 10^{-7} \left| \frac{g_{\Sigma_b^+ \rightarrow \overline{B}^0 p}}{5} \right|^2, \\ \mathcal{B}(B^- \rightarrow n\bar{p}) &= 5.0 \times 10^{-7} \left| \frac{g_{\Sigma_b^+ \rightarrow \overline{B}^0 p}}{5} \right|^2.\end{aligned}\quad (3.27)$$

3. $\overline{B}^0 \rightarrow \Lambda\bar{\Lambda}$

Let us consider the PC amplitude of $\overline{B}^0 \rightarrow \Lambda\bar{\Lambda}$. In the pole model it receives pole contributions from the anti-triplet Ξ_b^0 and sextet $\Xi_b^{\prime 0}$

$$B = \frac{g_{\Xi_b^0 \rightarrow \overline{B}^0 \Lambda} a_{\Xi_b^0 \Lambda}}{m_\Lambda - m_{\Xi_b^0}} + \frac{g_{\Xi_b^{\prime 0} \rightarrow \overline{B}^0 \Lambda} a_{\Xi_b^{\prime 0} \Lambda}}{m_\Lambda - m_{\Xi_b^{\prime 0}}}. \quad (3.28)$$

Using the wave functions given in Appendix A, we obtain

$$\begin{aligned}\langle \Lambda | O_1^{\text{PC}} | \Xi_b^0 \rangle &= -2X(4\pi), \\ \langle \Lambda | O_1^{\text{PC}} | \Xi_b^{\prime 0} \rangle &= -2\sqrt{3}X(4\pi),\end{aligned}\quad (3.29)$$

for PC matrix elements, and

$$g_{\Xi_b^0 \rightarrow \overline{B}^0 \Lambda} = -\sqrt{3} g_{\Xi_b^{\prime 0} \rightarrow \overline{B}^0 \Lambda} \quad (3.30)$$

for strong couplings. Then it is clear that the PC amplitude vanishes as the mass difference between Ξ_b and Ξ_b' is negligible. That is, this decay is purely parity violating in the 3P_0 quark-pair-creation model as noticed by Körner [5] and Jarfi *et al.* [10] some time ago. As noted in passing, we will not compute the PV amplitude within the framework of the bag model.

4. $B^- \rightarrow p\bar{\Delta}^{--}, n\bar{\Delta}^-, \overline{B}^0 \rightarrow p\bar{\Delta}^-, n\bar{\Delta}^0$

The relevant pole diagram consists of the intermediate states $\Sigma_b^{+(*)}$ for $p\bar{\Delta}^{--}, p\bar{\Delta}^-$ modes ($\bar{\Delta}^{--}$ being the antiparticle of Δ^{++} and likewise for other $\bar{\Delta}$ particles) and $\Sigma_b^{0(*)}$ as well as $\Lambda_b^{(*)}$ for $n\bar{\Delta}^-, n\bar{\Delta}^0$ final states. However, it is straightforward to show that, in the 3P_0 quark-pair-creation model, the strong coupling for $\Lambda_b \rightarrow N\bar{\Delta}$ vanishes and hence the Λ_b pole makes

no contribution. Moreover, the parity-violating part vanishes in the same quark-pair-creation model [5,10]. Therefore,

$$\begin{aligned} D(B^- \rightarrow p\bar{\Delta}^{--}) &= \frac{g_{\Sigma_b^+ \rightarrow B^- \Delta^{++}} a_{\Sigma_b^+ p}}{m_p - m_{\Sigma_b}}, & D(B^- \rightarrow n\bar{\Delta}^-) &= \frac{g_{\Sigma_b^0 \rightarrow B^- \Delta^+} a_{\Sigma_b^0 n}}{m_n - m_{\Sigma_b}}, \\ D(\bar{B}^0 \rightarrow p\bar{\Delta}^-) &= \frac{g_{\Sigma_b^+ \rightarrow \bar{B}^0 \Delta^+} a_{\Sigma_b^+ p}}{m_p - m_{\Sigma_b}}, & D(\bar{B}^0 \rightarrow n\bar{\Delta}^0) &= \frac{g_{\Sigma_b^0 \rightarrow \bar{B}^0 \Delta^0} a_{\Sigma_b^0 n}}{m_n - m_{\Sigma_b}}, \end{aligned} \quad (3.31)$$

where the PC matrix elements $a_{\Sigma_b^+ p}$ and $a_{\Sigma_b^0 n}$ have been evaluated before. The relative strong couplings are

$$\begin{aligned} g_{\Sigma_b^+ \rightarrow B^- \Delta^{++}} &= -\sqrt{3} g_{\Sigma_b^+ \rightarrow \bar{B}^0 \Delta^+} = -\sqrt{3/2} g_{\Sigma_b^0 \rightarrow \bar{B}^0 \Delta^0} \\ &= \sqrt{3/2} g_{\Sigma_b^0 \rightarrow B^- \Delta^+} = 2\sqrt{6} g_{\Sigma_b^+ \rightarrow \bar{B}^0 p}. \end{aligned} \quad (3.32)$$

This together with the baryon matrix elements (3.9) and (3.16) leads to the relation

$$\Gamma(B^- \rightarrow p\bar{\Delta}^{--}) = 3\Gamma(B^- \rightarrow n\bar{\Delta}^-) = 3\Gamma(\bar{B}^0 \rightarrow p\bar{\Delta}^-) = 3\Gamma(\bar{B}^0 \rightarrow n\bar{\Delta}^0), \quad (3.33)$$

as first pointed out by Jarfi *et al.* [10]. In the diquark model of [11], $n\bar{\Delta}^-$ has a rate different from $p\bar{\Delta}^-$ and $n\bar{\Delta}^0$. Hence, experimentally it is important to test the relation (3.33).

If we apply Eq. (3.32) and use $|g_{\Sigma_b^+ \rightarrow \bar{B}^0 p}| = 5$, we will obtain $|g_{\Sigma_b^+ \rightarrow B^- \Delta^{++}}| = 24$ and $\mathcal{B}(B^- \rightarrow p\bar{\Delta}^{--}) = 5.8 \times 10^{-6}$. Because of the strong decay $\bar{\Delta}^{--} \rightarrow p\bar{\pi}^-$, the resonant contribution from $\bar{\Delta}^{--}$ to the branching ratio of $p\bar{p}\pi^-$ would be 6×10^{-6} . This already exceeds the recent Belle measurement $\mathcal{B}(B^- \rightarrow p\bar{p}\pi^-) = (1.9_{-0.9}^{+1.0} \pm 0.3) \times 10^{-6}$ or the upper limit of $\mathcal{B}(B^- \rightarrow p\bar{p}\pi^-) < 3.7 \times 10^{-6}$ [23]. Therefore, the coupling of the Δ to the B meson and the octet baryon is smaller than what is expected from Eq. (3.32) probably due to the different off-shellness of Δ . Recall that the parity-conserving transition to the Δ corresponds to a $L = 2$ partial wave. Therefore, the off-shell suppression on the three-point coupling of $\Sigma_b \rightarrow B\Delta$ is likely to be different from that of $\Lambda_b \rightarrow BN$. For definiteness, we will choose $|g_{\Sigma_b^+ \rightarrow B^- \Delta^{++}}| = 12$ and obtain

$$\mathcal{B}(B^- \rightarrow p\bar{\Delta}^{--}) = 1.4 \times 10^{-6} \left| \frac{g_{\Sigma_b^+ \rightarrow B^- \Delta^{++}}}{12} \right|^2. \quad (3.34)$$

Thus this charmless decay $B^- \rightarrow p\bar{\Delta}^{--}$ can have a large branching ratio of order 10^{-6} owing to the large coupling constant $g_{\Sigma_b^+ \rightarrow B^- \Delta^{++}}$. In sharp contrast, this mode is predicted to be only at the level of 3×10^{-7} in the QCD sum rule analysis [7] (see also Table II). The branching ratios of other modes can be calculated using Eq. (3.33) and are shown in Table II. Experimentally, the decay $B^- \rightarrow p\bar{\Delta}^{--}$ should be readily accessible by B factories BaBar and Belle.

B. Penguin-dominated two-body decays

1. $B^- \rightarrow \Lambda \bar{p}$, $\bar{B}^0 \rightarrow \Lambda \bar{n}$

This decay receives internal W -emission and $b \rightarrow s$ penguin contributions [see Fig. 1(a)]. As we shall see below, it is a penguin-dominated mode. The pole diagram for $B^- \rightarrow \Lambda \bar{p}$ consists of the intermediate states $\Lambda_b^{0(*)}$ and $\Sigma_b^{0(*)}$

$$A = -\frac{g_{\Lambda_b^* \rightarrow B^- p} b_{\Lambda_b^* \Lambda}}{m_\Lambda - m_{\Lambda_b^*}} - \frac{g_{\Sigma_b^{0*} \rightarrow B^- p} b_{\Sigma_b^{0*} \Lambda}}{m_\Lambda - m_{\Sigma_b^*}}, \quad B = \frac{g_{\Lambda_b \rightarrow B^- p} a_{\Lambda_b \Lambda}}{m_\Lambda - m_{\Lambda_b}} + \frac{g_{\Sigma_b^0 \rightarrow B^- p} a_{\Sigma_b^0 \Lambda}}{m_\Lambda - m_{\Sigma_b}}. \quad (3.35)$$

To evaluate the hadronic matrix elements, we notice that the combinations of the operators $O_{2i+1} + O_{2i+2}$ ($i = 0, \dots, 4$) are symmetric in color indices and hence they cannot contribute to the baryon-baryon matrix element. From this we can write the PC matrix element $a_{\Lambda_b \Lambda}$ as

$$a_{\Lambda_b \Lambda} = \frac{G_F}{\sqrt{2}} \left\{ V_{ub} V_{us}^* (c_1^{\text{eff}} - c_2^{\text{eff}}) \langle \Lambda | O_1^{\text{PC}} | \Lambda_b \rangle - V_{tb} V_{ts}^* [(c_3^{\text{eff}} - c_4^{\text{eff}}) \langle \Lambda | O_3^{\text{PC}} | \Lambda_b \rangle + (c_5^{\text{eff}} - c_6^{\text{eff}}) \langle \Lambda | O_5^{\text{PC}} | \Lambda_b \rangle + (c_7^{\text{eff}} - c_8^{\text{eff}}) \langle \Lambda | O_7^{\text{PC}} | \Lambda_b \rangle + (c_9^{\text{eff}} - c_{10}^{\text{eff}}) \langle \Lambda | O_9^{\text{PC}} | \Lambda_b \rangle] \right\}. \quad (3.36)$$

Since the bag model implies

$$\langle \Lambda | (\bar{s}b)_{V-A} (\bar{d}d)_{V\pm A} | \Lambda_b \rangle_{\text{PC}} = \langle \Lambda | (\bar{s}b)_{V-A} (\bar{u}u)_{V\pm A} | \Lambda_b \rangle_{\text{PC}}, \quad (3.37)$$

the baryon matrix elements of O_3 and O_9 can be related to O_1 , while matrix element of O_7 is related to O_5 , for example,

$$\langle \Lambda | O_3^{\text{PC}} | \Lambda_b \rangle = \langle \Lambda | (\bar{s}b)_{V-A} [(\bar{u}u)_{V-A} + (\bar{d}d)_{V-A}] | \Lambda_b \rangle_{\text{PC}} = -2 \langle \Lambda | O_1^{\text{PC}} | \Lambda_b \rangle. \quad (3.38)$$

Hence, Eq. (3.36) can be recast as

$$a_{\Lambda_b \Lambda} = \frac{G_F}{\sqrt{2}} \left\{ \left[V_{ub} V_{us}^* (c_1^{\text{eff}} - c_2^{\text{eff}}) - V_{tb} V_{ts}^* \left(-2c_3^{\text{eff}} + 2c_4^{\text{eff}} - \frac{1}{2}c_9^{\text{eff}} + \frac{1}{2}c_{10}^{\text{eff}} \right) \right] \langle \Lambda | O_1^{\text{PC}} | \Lambda_b \rangle - V_{tb} V_{ts}^* (c_5^{\text{eff}} - c_6^{\text{eff}} + \frac{1}{2}c_7^{\text{eff}} - \frac{1}{2}c_8^{\text{eff}}) \langle \Lambda | O_5^{\text{PC}} | \Lambda_b \rangle \right\}. \quad (3.39)$$

Likewise, the relation

$$\langle \Lambda | (\bar{s}b)_{V-A} (\bar{d}d)_{V\pm A} | \Sigma_b^0 \rangle_{\text{PC}} = -\langle \Lambda | (\bar{s}b)_{V-A} (\bar{u}u)_{V\pm A} | \Sigma_b^0 \rangle_{\text{PC}} \quad (3.40)$$

implied by the bag model leads to

$$a_{\Sigma_b^0 \Lambda} = \frac{G_F}{\sqrt{2}} \left\{ \left[V_{ub} V_{us}^* (c_1^{\text{eff}} - c_2^{\text{eff}}) - V_{tb} V_{ts}^* \left(-\frac{3}{2}c_9^{\text{eff}} + \frac{3}{2}c_{10}^{\text{eff}} \right) \right] \langle \Lambda | O_1^{\text{PC}} | \Sigma_b^0 \rangle - V_{tb} V_{ts}^* (c_7^{\text{eff}} - c_8^{\text{eff}}) \langle \Lambda | O_7^{\text{PC}} | \Sigma_b^0 \rangle \right\}. \quad (3.41)$$

Therefore, the PC matrix element for $\Sigma_b^0 - \Lambda$ weak transition does not receive QCD penguin contributions.

Applying Eqs. (B2) and (B5) we obtain

$$\begin{aligned}\langle \Lambda | O_1^{\text{PC}} | \Lambda_b \rangle &= \frac{4}{3} X_1(4\pi), \\ \langle \Lambda | O_5^{\text{PC}} | \Lambda_b \rangle &= \frac{4}{3} (2Y_1 + 2Y_2 - Y'_1 + Y'_2)(4\pi), \\ \langle \Lambda | O_1^{\text{PC}} | \Sigma_b^0 \rangle &= -\frac{1}{\sqrt{3}} (X_1 + 3X_2)(4\pi), \\ \langle \Lambda | O_7^{\text{PC}} | \Sigma_b^0 \rangle &= -\frac{\sqrt{3}}{2} [Y_1 + Y_2 - 2(Y'_1 - Y'_2)](4\pi),\end{aligned}\tag{3.42}$$

in the bag model, where

$$\begin{aligned}X_1 &= \int_0^R r^2 dr [u_s(r)v_u(r) - v_s(r)u_u(r)][u_u(r)v_b(r) - v_u(r)u_b(r)], \\ X_2 &= \int_0^R r^2 dr [u_s(r)u_u(r) + v_s(r)v_u(r)][u_u(r)u_b(r) + v_u(r)v_b(r)], \\ Y_1 &= \int_0^R r^2 dr [u_s(r)v_b(r) - v_s(r)u_b(r)][u_u(r)v_u(r) - v_u(r)u_u(r)], \\ Y'_1 &= \int_0^R r^2 dr [u_s(r)v_b(r) + v_s(r)u_b(r)][u_u(r)v_u(r) + v_u(r)u_u(r)], \\ Y_2 &= \int_0^R r^2 dr [u_s(r)u_b(r) + v_s(r)v_b(r)][u_u(r)u_u(r) + v_u(r)v_u(r)], \\ Y'_2 &= \int_0^R r^2 dr [u_s(r)u_b(r) - v_s(r)v_b(r)][u_u(r)u_u(r) - v_u(r)v_u(r)],\end{aligned}\tag{3.43}$$

are four-quark overlap bag integrals. Finally we arrive at

$$B(B^- \rightarrow \Lambda \bar{p}) = -\frac{1}{\sqrt{2}} g_{\Sigma_b^+ \rightarrow \bar{B}^0 p} \left(\frac{3\sqrt{3} a_{\Lambda_b \Lambda}}{m_\Lambda - m_{\Lambda_b}} + \frac{a_{\Sigma_b^0 \Lambda}}{m_\Lambda - m_{\Sigma_b}} \right),\tag{3.44}$$

where use has been made of Eqs. (3.23) and (3.24).

The bag integrals have the values

$$\begin{aligned}X_1 &= -4.6 \times 10^{-6} \text{ GeV}^3, & X_2 &= 1.7 \times 10^{-4} \text{ GeV}^3, & Y_1 &= 0, \\ Y'_1 &= 4.5 \times 10^{-5} \text{ GeV}^3, & Y_2 &= 1.7 \times 10^{-4} \text{ GeV}^3, & Y'_2 &= 1.2 \times 10^{-4} \text{ GeV}^3.\end{aligned}\tag{3.45}$$

It is easy to check that $a_{\Lambda_b \Lambda}$ and hence the decay is penguin dominated. For the branching ratio we find

$$\mathcal{B}(B^- \rightarrow \Lambda \bar{p})_{\text{PC}} = 2.2 \times 10^{-7} \left| \frac{g_{\Sigma_b^+ \rightarrow \bar{B}^0 p}}{5} \right|^2.\tag{3.46}$$

For $\bar{B}^0 \rightarrow \Lambda \bar{n}$, it has the same rate as $B^- \rightarrow \Lambda \bar{p}$.

2. $\overline{B}^0 \rightarrow \Sigma^+ \bar{p}$

We consider the pole diagram with the intermediate states $\Sigma_b^{+(*)}$

$$A = -\frac{g_{\Sigma_b^{+*} \rightarrow \overline{B}^0 p} b_{\Sigma_b^{*p}}}{m_\Sigma - m_{\Sigma_b^*}}, \quad B = \frac{g_{\Sigma_b^+ \rightarrow \overline{B}^0 p} a_{\Sigma_b^+ \Sigma}}{m_\Sigma - m_{\Sigma_b^+}}. \quad (3.47)$$

The PC weak matrix element for $\Sigma_b^+ - \Sigma^+$ transition reads

$$a_{\Sigma_b^+ \Sigma^+} = \frac{G_F}{\sqrt{2}} \left\{ \left[V_{ub} V_{us}^* (c_1^{\text{eff}} - c_2^{\text{eff}}) - V_{tb} V_{ts}^* (-c_3^{\text{eff}} + c_4^{\text{eff}} - c_9^{\text{eff}} + c_{10}^{\text{eff}}) \right] \langle \Sigma^+ | O_1^{\text{PC}} | \Sigma_b^+ \rangle \right. \\ \left. - V_{tb} V_{ts}^* (c_5^{\text{eff}} - c_6^{\text{eff}} + c_7^{\text{eff}} - c_8^{\text{eff}}) \langle \Sigma^+ | O_5^{\text{PC}} | \Sigma_b^+ \rangle \right\}. \quad (3.48)$$

In the bag model,

$$\langle \Sigma^+ | O_1^{\text{PC}} | \Sigma_b^+ \rangle = \frac{2}{3} (X_1 - 9X_2) (4\pi), \\ \langle \Sigma^+ | O_5^{\text{PC}} | \Sigma_b^+ \rangle = \frac{2}{3} [Y_1 + Y_2 + 4(Y'_1 - Y'_2)] (4\pi). \quad (3.49)$$

We obtain numerically

$$\mathcal{B}(\overline{B}^0 \rightarrow \Sigma^+ \bar{p})_{\text{PC}} = 1.8 \times 10^{-8} \left| \frac{g_{\Sigma_b^+ \rightarrow \overline{B}^0 p}}{5} \right|^2. \quad (3.50)$$

Note that the branching ratio is predicted to be 5×10^{-6} in the QCD sum rule analysis of [7], which is larger than our result by two orders of magnitude (see Table II).

3. $B^- \rightarrow \Sigma^0 \bar{p}$

The intermediate low-lying pole states for this decay are $\Lambda_b^{0(*)}$ and $\Sigma_b^{0(*)}$

$$A = -\frac{g_{\Lambda_b^* \rightarrow B^- p} b_{\Lambda_b^* \Sigma^0}}{m_\Sigma - m_{\Lambda_b^*}} - \frac{g_{\Sigma_b^{0*} \rightarrow B^- p} b_{\Sigma_b^{0*} \Sigma^0}}{m_\Sigma - m_{\Sigma_b^*}}, \quad B = \frac{g_{\Lambda_b \rightarrow B^- p} a_{\Lambda_b \Sigma^0}}{m_\Sigma - m_{\Lambda_b}} + \frac{g_{\Sigma_b^0 \rightarrow B^- p} a_{\Sigma_b^0 \Sigma^0}}{m_\Sigma - m_{\Sigma_b}}. \quad (3.51)$$

The PC matrix elements are given by

$$a_{\Sigma_b^0 \Sigma^0} = \frac{G_F}{\sqrt{2}} \left\{ \left[V_{ub} V_{us}^* (c_1^{\text{eff}} - c_2^{\text{eff}}) - V_{tb} V_{ts}^* (-2c_3^{\text{eff}} + 2c_4^{\text{eff}} - \frac{1}{2}c_9^{\text{eff}} + \frac{1}{2}c_{10}^{\text{eff}}) \right] \langle \Sigma^0 | O_1^{\text{PC}} | \Sigma_b^0 \rangle \right. \\ \left. - V_{tb} V_{ts}^* (c_5^{\text{eff}} - c_6^{\text{eff}} + \frac{1}{2}c_7^{\text{eff}} - \frac{1}{2}c_8^{\text{eff}}) \langle \Sigma^0 | O_5^{\text{PC}} | \Sigma_b^0 \rangle \right\}, \quad (3.52)$$

and

$$a_{\Lambda_b^0 \Sigma^0} = \frac{G_F}{\sqrt{2}} \left\{ \left[V_{ub} V_{us}^* (c_1^{\text{eff}} - c_2^{\text{eff}}) - V_{tb} V_{ts}^* (-\frac{3}{2}c_9^{\text{eff}} + \frac{3}{2}c_{10}^{\text{eff}}) \right] \langle \Sigma^0 | O_1^{\text{PC}} | \Lambda_b \rangle \right. \\ \left. - V_{tb} V_{ts}^* (c_7^{\text{eff}} - c_8^{\text{eff}}) \langle \Sigma^0 | O_7^{\text{PC}} | \Lambda_b \rangle \right\}, \quad (3.53)$$

where in the bag model

$$\begin{aligned}
\langle \Sigma^0 | O_1^{\text{PC}} | \Lambda_b \rangle &= -\frac{1}{\sqrt{3}}(X_1 + 3X_2)(4\pi), \\
\langle \Sigma^0 | O_7^{\text{PC}} | \Lambda_b \rangle &= -\frac{\sqrt{3}}{2}[Y_1 + Y_2 - 2(Y'_1 - Y'_2)](4\pi), \\
\langle \Sigma^0 | O_1^{\text{PC}} | \Sigma_b^0 \rangle &= \frac{1}{3}(X_1 - 9X_2)(4\pi), \\
\langle \Sigma^0 | O_5^{\text{PC}} | \Sigma_b^0 \rangle &= \frac{2}{3}[Y_1 + Y_2 + 4(Y'_1 - Y'_2)](4\pi).
\end{aligned} \tag{3.54}$$

Hence,

$$B = -\frac{1}{\sqrt{2}}g_{\Sigma_b^+ \rightarrow \bar{B}^0 p} \left(\frac{3\sqrt{3}a_{\Lambda_b \Sigma^0}}{m_\Sigma - m_{\Lambda_b}} + \frac{a_{\Sigma_b^0 \Sigma^0}}{m_\Sigma - m_{\Sigma_b}} \right), \tag{3.55}$$

where use of Eqs. (3.23) and (3.24) for strong couplings has been made. We obtain

$$\mathcal{B}(B^- \rightarrow \Sigma^0 \bar{p})_{\text{PC}} = 5.8 \times 10^{-8} \left| \frac{g_{\Sigma_b^+ \rightarrow \bar{B}^0 p}}{5} \right|^2. \tag{3.56}$$

Again, the QCD sum rule prediction for this mode is much higher [7].

4. $B^- \rightarrow \Sigma^+ \bar{\Delta}^{--}$, $\Sigma^- \bar{\Delta}^0$, $\bar{B}^0 \rightarrow \Sigma^+ \bar{\Delta}^-$

As stated before, the decays $B^- \rightarrow \Sigma^+ \bar{\Delta}^{--}$, $\Sigma^- \bar{\Delta}^0$, $\bar{B}^0 \rightarrow \Sigma^+ \bar{\Delta}^-$ only receive parity-conserving contributions [5,10] so that

$$\begin{aligned}
D(B^- \rightarrow \Sigma^+ \bar{\Delta}^{--}) &= \frac{g_{\Sigma_b^+ \rightarrow B^- \Delta^{++}} a_{\Sigma_b^+ \Sigma^+}}{m_\Sigma - m_{\Sigma_b}}, \\
D(\bar{B}^0 \rightarrow \Sigma^+ \bar{\Delta}^-) &= \frac{g_{\Sigma_b^+ \rightarrow \bar{B}^0 \Delta^+} a_{\Sigma_b^+ \Sigma^+}}{m_\Sigma - m_{\Sigma_b}}, \\
D(B^- \rightarrow \Sigma^- \bar{\Delta}^0) &= \frac{g_{\Sigma_b^- \rightarrow B^- \Delta^0} a_{\Sigma_b^- \Sigma^-}}{m_\Sigma - m_{\Sigma_b}}.
\end{aligned} \tag{3.57}$$

The PC matrix element $a_{\Sigma_b^+ \Sigma^+}$ has been evaluated before and $a_{\Sigma_b^- \Sigma^-} = a_{\Sigma_b^+ \Sigma^+}$. For strong couplings we get

$$g_{\Sigma_b^+ \rightarrow \Delta^{++} B^-} = -\sqrt{3} g_{\Sigma_b^+ \rightarrow \Delta^+ \bar{B}^0} = \sqrt{3} g_{\Sigma_b^- \rightarrow \Delta^0 B^-} = 2\sqrt{6} g_{\Sigma_b^+ \rightarrow p \bar{B}^0}, \tag{3.58}$$

in the 3P_0 model. Collecting all the results gives

$$\begin{aligned}
\mathcal{B}(B^- \rightarrow \Sigma^+ \bar{\Delta}^{--}) &= 2.0 \times 10^{-7} \left| \frac{g_{\Sigma_b^+ \rightarrow \Delta^{++} B^-}}{12} \right|^2, \\
\mathcal{B}(\bar{B}^0 \rightarrow \Sigma^+ \bar{\Delta}^-) &= 6.3 \times 10^{-8} \left| \frac{g_{\Sigma_b^+ \rightarrow \Delta^{++} B^-}}{12} \right|^2, \\
\mathcal{B}(B^- \rightarrow \Sigma^- \bar{\Delta}^0) &= 8.7 \times 10^{-8} \left| \frac{g_{\Sigma_b^+ \rightarrow \Delta^{++} B^-}}{12} \right|^2,
\end{aligned} \tag{3.59}$$

where we have followed the discussion of $\bar{B} \rightarrow N \bar{\Delta}$ to choose the coupling $|g_{\Sigma_b^+ \rightarrow \Delta^{++} B^-}| = 12$ as a benchmarked value.

C. Comparison with other models

As discussed in passing, though we adopt the same pole-model framework as Jarfi *et al.* [10] for describing two-body baryonic B decays, a crucial difference is that weak baryon matrix elements are evaluated by Jarfi *et al.* at large momentum transfer and strong couplings at small transfer, whereas the weak transition is computed at zero transfer and strong couplings at large momentum transfer in our case. In general, the difference in numerical results shown in Table II comes mainly from the fact that we use the bag model rather than the harmonic oscillator model to evaluate weak baryon transitions.

In the following we compare our results with the diquark model by Ball and Dosch [11] and the QCD sum rule analysis by Chernyak and Zhitnitsky [7] (see also Table II). For $\bar{B} \rightarrow N\bar{N}$ decays, the diquark model has one unique prediction, namely, there is no $B^- \rightarrow n\bar{p}$ decay, while $p\bar{p}$ and $n\bar{n}$ final states have the same rates. In contrast, the sum rule approach predicts that $\Gamma(\bar{B}^0 \rightarrow p\bar{p}) > \Gamma(B^- \rightarrow n\bar{p}) > \Gamma(\bar{B}^0 \rightarrow n\bar{n})$ (see Table II), while in our case $\Gamma(B^- \rightarrow n\bar{p}) > \Gamma(\bar{B}^0 \rightarrow p\bar{p}) \approx \Gamma(\bar{B}^0 \rightarrow n\bar{n})$. Therefore, a measurement of the relative rates of $\bar{B} \rightarrow N\bar{N}$ (especially $B^- \rightarrow n\bar{p}$) will serve to test the three models.

As for the tree-dominated modes $\bar{B} \rightarrow N\bar{\Delta}$, they are suppressed in the diquark model because the operators O_1 and O_2 can only generate scalar diquarks whereas the decuplet baryons are made of a vector diquark and a quark. Likewise, they are also suppressed in the sum rule analysis. In sharp contrast, these modes have sizable branching ratios in the pole model, namely, $\Gamma(\bar{B} \rightarrow N\bar{\Delta}) > \Gamma(\bar{B} \rightarrow N\bar{N})$, owing to the large coupling of the intermediate state Σ_b with the B meson and the Δ resonance.

The penguin-dominated decays have smaller rates than $\bar{B} \rightarrow p\bar{p}$ in the diquark model as the penguin operators are not included in the original calculations by Ball and Dosch (the effect of the penguin operators in this model was recently discussed in [33]). In contrast, the sum rule approach predicts branching ratios of order $(2 - 6) \times 10^{-6}$ for $\bar{B} \rightarrow \Lambda\bar{p}$, $\Sigma\bar{p}$, $\Sigma\bar{\Delta}$. In our work, the decay rates of penguin-dominated decays are in general small.

In short, measurements of the relative rates of $\bar{B} \rightarrow N\bar{N}$, $\Sigma\bar{p}$, $\Sigma\bar{\Delta}$ will suffice to differentiate between above-mentioned three models.

IV. CHARMLESS THREE-BODY BARYONIC DECAYS

As noted in the Introduction, the study and search of the three-body baryonic B decay $\bar{B} \rightarrow \mathcal{B}_1\bar{\mathcal{B}}_2 M$ with M being a meson are mainly motivated by the experimental observation that $\mathcal{B}(B^- \rightarrow \Lambda_c\bar{p}\pi^-) > \mathcal{B}(\bar{B}^0 \rightarrow \Lambda_c\bar{p})$ [22] and $\mathcal{B}(B^- \rightarrow p\bar{p}K^-) > \mathcal{B}(\bar{B}^0 \rightarrow p\bar{p})$ [23]. Theoretically, it has been argued that the emitted meson M in the three-body final state carries away much energies and the configuration is more favorable for baryon production because of reduced energy release compared to the latter [18]. Roughly speaking, the reason that the two-body baryonic decay $B \rightarrow \mathcal{B}_1\bar{\mathcal{B}}_2$ is smaller than the mesonic counterpart $B \rightarrow M_1\bar{M}_2$ stems from the fact that one needs an additional quark pair production in the internal

W -emission diagram [Fig. 1(a)] and two $q\bar{q}$ pairs in weak annihilation diagrams [Fig. 1(b)] in order to form a baryon-antibaryon pair. A $q\bar{q}$ production is suppressed by either a strong coupling when it is produced perturbatively via one gluon exchange or by intrinsic softness of nonperturbative pair creation [17]. In the three-body baryonic decay, the emission of the meson M will carry away energies in such a way that the invariant mass of $\mathcal{B}_1\bar{\mathcal{B}}_2$ becomes smaller and hence it is relatively easier to fragment into the baryon-antibaryon pair.

One can also understand the above feature more concretely by studying the Dalitz plot. Due to the $V - A$ nature of the $b \rightarrow ud\bar{u}$ process, the invariant mass of the diquark ud peaks at the highest possible values in a Dalitz plot for $b \rightarrow udd\bar{d}$ transition (see [34] and footnote [91] in [35]). If the ud forms a nucleon, then the very massive udq objects will intend to form a highly excited baryon state such as Δ and N^* and will be seen as $Nn\pi (n \geq 1)$ [16]. This explains the non-observation of the $N\bar{N}$ final states and why the three-body mode $N\bar{N}\pi(\rho)$ is favored. Of course, this does not necessarily imply that the three-body final state $\mathcal{B}_1\bar{\mathcal{B}}_2M$ always has a larger rate than the two-body one $\mathcal{B}_1\bar{\mathcal{B}}_2$. In this section we will study some leading charmless three-body baryonic B decays and see under what condition that the above argument holds.

The quark diagrams and the corresponding pole diagrams for decays of B mesons to the baryonic final state $\mathcal{B}_1\bar{\mathcal{B}}_2M$ are more complicated. In general there are two external W -diagrams Figs. 2(a)-2(b), four internal W -emissions Figs. 2(c)-2(f), and one W -exchange Fig. 2(g) for the neutral B meson and one W -annihilation Fig. 2(h) for the charged B . Because of space limit, penguin diagrams are not drawn in Fig. 2; they can be obtained from Figs. 2(c)-2(g) by replacing the $b \rightarrow u$ tree transition by the $b \rightarrow s(d)$ penguin transition. Under the factorization hypothesis, the relevant factorizable amplitudes are

$$\begin{aligned} \text{Figs. 2(a), 2(c)} : \mathcal{A} &\propto \langle M | (\bar{q}_3 q_2) | 0 \rangle \langle \mathcal{B}_1 \bar{\mathcal{B}}_2 | (\bar{q}_1 b) | B \rangle, \\ \text{Figs. 2(b), 2(d)} : \mathcal{A} &\propto \langle \mathcal{B}_1 \bar{\mathcal{B}}_2 | (\bar{q}_1 q_2) | 0 \rangle \langle M | (\bar{q}_3 b) | B \rangle, \\ \text{Figs. 2(g), 2(h)} : \mathcal{A} &\propto \langle \mathcal{B}_1 \bar{\mathcal{B}}_2 M | (\bar{q}_1 q_2) | 0 \rangle \langle 0 | (\bar{q}_3 b) | B \rangle. \end{aligned} \quad (4.1)$$

Since the three-body matrix elements are basically unknown, only the factorizable amplitudes for Fig. 2(b) or 2(d) are calculable in practice.

The tree-dominated three-body modes of interest are:

$$\begin{aligned} \bar{B}^0 &\rightarrow \pi^+(\rho^+) \{ n\bar{p}, \Lambda\bar{\Sigma}^-, \Sigma^0\bar{\Sigma}^-, \Sigma^-\bar{\Lambda}, \Xi^-\bar{\Xi}^0, p\bar{\Delta}^{--}, \dots \}, \\ \bar{B}^0 &\rightarrow \pi^-(\rho^-) \{ p\bar{n}, \Sigma^+\bar{\Lambda}, \Sigma^+\bar{\Sigma}^0, \Lambda\bar{\Sigma}^+, \Delta^{++}\bar{p}, \dots \}, \\ B^- &\rightarrow \pi^-(\rho^-) \{ p\bar{p}, n\bar{n}, \Sigma\bar{\Sigma}, \Lambda\bar{\Lambda}, \Delta\bar{\Delta}, \dots \}, \end{aligned} \quad (4.2)$$

while some interesting penguin-dominated decays are

$$\begin{aligned} \bar{B}^0 &\rightarrow \pi^+(\rho^+) \{ \Lambda\bar{p}, \Sigma^0\bar{p}, \Sigma^-\bar{n}, \Xi^-\bar{\Lambda}, \Sigma^+\bar{\Delta}^{--}, \dots \}, \\ B^- &\rightarrow \pi^-(\rho^-) \{ \Sigma^+\bar{p}, \Lambda\bar{n}, \Sigma^0\bar{n}, \Xi^0\bar{\Lambda}, \Sigma^+\bar{\Delta}^-, \dots \}, \\ \bar{B}^0 &\rightarrow K^{-(*)} \{ p\bar{n}, \Sigma^+\bar{\Lambda}, \Sigma^+\bar{\Sigma}^0, \Lambda\bar{\Sigma}^+, \Xi^0\bar{\Xi}^+, \Delta^{++}\bar{p}, \dots \}, \end{aligned} \quad (4.3)$$

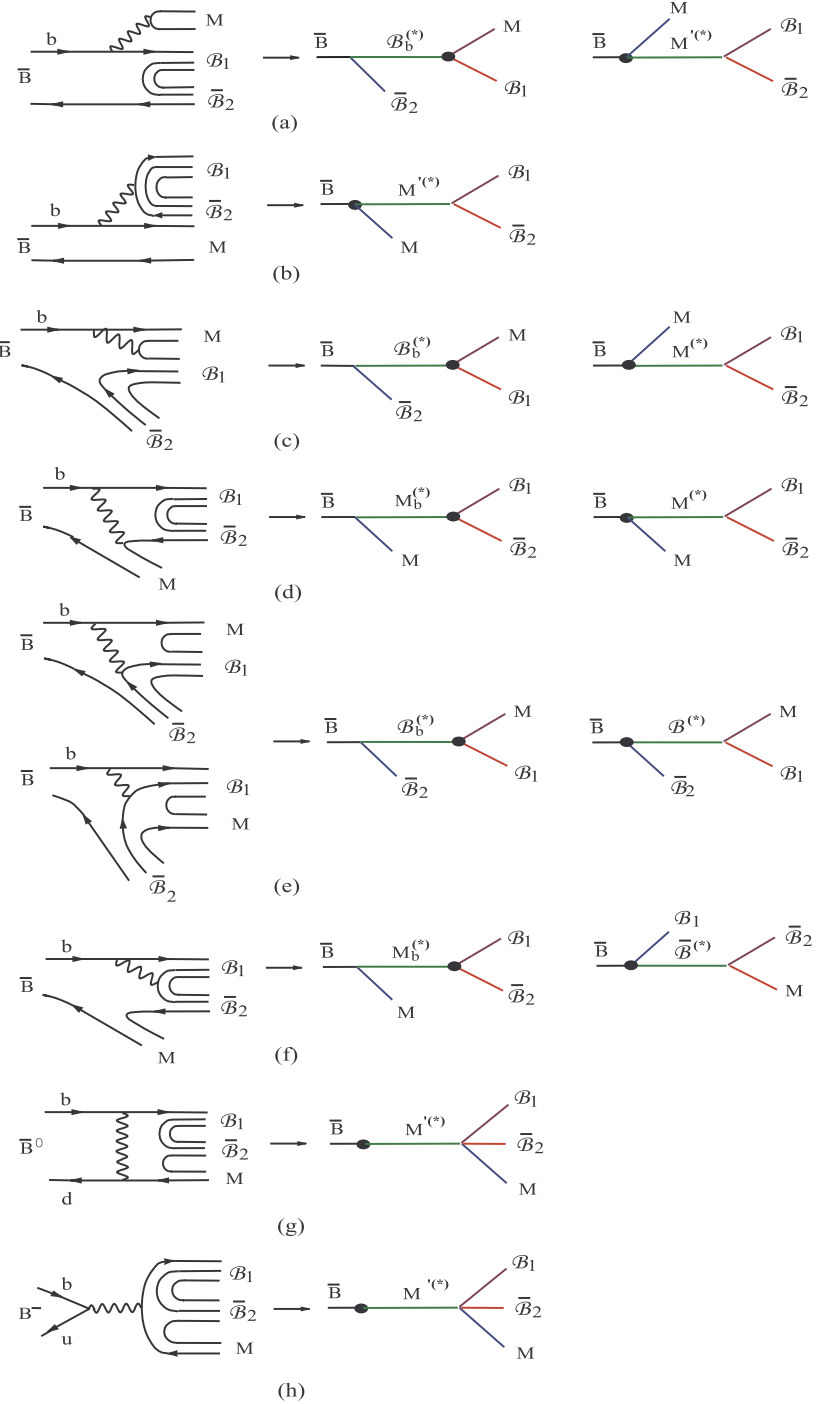


FIG. 2. Quark and pole diagrams for three-body baryonic B decay $\bar{B} \rightarrow \mathcal{B}_1 \bar{\mathcal{B}}_2 M$, where the symbol \bullet denotes the weak vertex. Figs. 2(a) and 2(b) correspond to factorizable external W -emission contributions, Figs. 2(c) and 2(d) to factorizable internal W -emission, Figs. 2(e) and 2(f) to nonfactorizable internal W -emission, Fig. 2(g) to W -exchange and Fig. 2(h) to W -annihilation. Penguin contributions are obtained from Figs. 2(c)-2(g) by replacing the $b \rightarrow u$ tree transition by the $b \rightarrow s(d)$ penguin transition.

$$\begin{aligned}
B^- &\rightarrow K^{-(*)} \{ p\bar{p}, n\bar{n}, \Sigma\bar{\Sigma}, \Lambda\bar{\Lambda}, \Delta\bar{\Delta}, \dots \}, \\
\overline{B}^0 &\rightarrow \overline{K}^{0(*)} \{ p\bar{p}, n\bar{n}, \Sigma\bar{\Sigma}, \Lambda\bar{\Lambda}, \Delta\bar{\Delta}, \dots \}, \\
B^- &\rightarrow \overline{K}^{0(*)} \{ n\bar{p}, \Lambda\bar{\Sigma}^-, \Sigma^0\bar{\Sigma}^-, \Sigma^-\bar{\Lambda}, p\bar{\Delta}^{--}, \dots \}.
\end{aligned}$$

In the present paper we will focus on octet baryon final states.

To evaluate the factorizable amplitude for Fig. 2(b) or 2(d) we need to know the octet baryon form factors defined by

$$\begin{aligned}
\langle \mathcal{B}_1(p_1) \overline{\mathcal{B}}_2(p_2) | (V \pm A)_\mu | 0 \rangle = \bar{u}_1(p_1) & \left\{ f_1^{\mathcal{B}_1\mathcal{B}_2}(q^2) \gamma_\mu + i \frac{f_2^{\mathcal{B}_1\mathcal{B}_2}(q^2)}{m_1 + m_2} \sigma_{\mu\nu} q^\nu + \frac{f_3^{\mathcal{B}_1\mathcal{B}_2}(q^2)}{m_1 + m_2} q_\mu \right. \\
& \left. \pm \left[g_1^{\mathcal{B}_1\mathcal{B}_2}(q^2) \gamma_\mu + i \frac{g_2^{\mathcal{B}_1\mathcal{B}_2}(q^2)}{m_1 + m_2} \sigma_{\mu\nu} q^\nu + \frac{g_3^{\mathcal{B}_1\mathcal{B}_2}(q^2)}{m_1 + m_2} q_\mu \right] \gamma_5 \right\} v_2(p_2), \quad (4.4)
\end{aligned}$$

where $q = p_1 + p_2$. For octet baryons one can apply SU(3) symmetry to relate the vector form factors $f_i^{\mathcal{B}_1\mathcal{B}_2}$ to the nucleon magnetic and electric form factors. In general, SU(3) symmetry implies

$$f_i^{\mathcal{B}_1\mathcal{B}_2}(q^2) = d^{\mathcal{B}_1\mathcal{B}_2} D_i^V(q^2) + f^{\mathcal{B}_1\mathcal{B}_2} F_i^V(q^2), \quad g_i^{\mathcal{B}_1\mathcal{B}_2}(q^2) = d^{\mathcal{B}_1\mathcal{B}_2} D_i^A(q^2) + f^{\mathcal{B}_1\mathcal{B}_2} F_i^A(q^2), \quad (4.5)$$

where $d^{\mathcal{B}_1\mathcal{B}_2}$ and $f^{\mathcal{B}_1\mathcal{B}_2}$ are the well-known Clebsch-Gordon coefficients and $F_i^V(q^2)$ and $D_i^V(q^2)$ are reduced form factors. The nucleon matrix element of the electromagnetic current is given by

$$\langle N(p_1) \overline{N}(p_2) | J_\mu^{\text{em}} | 0 \rangle = \bar{u}_N(p_1) \left[F_1(q^2) \gamma_\mu + i \frac{F_2(q^2)}{2m_N} \sigma_{\mu\nu} q^\nu \right] v_{\bar{N}}(p_2). \quad (4.6)$$

Since $J_\mu^{\text{em}} = V_\mu^3 + \frac{1}{\sqrt{3}} V_\mu^8$, SU(3) symmetry allows us to determine $F_i^V(q^2)$ and $D_i^V(q^2)$ separately. The results are (see e.g. [36])

$$F_{1,2}^V(t) = F_{1,2}^p(t) + \frac{1}{2} F_{1,2}^n(t), \quad D_{1,2}^V(t) = -\frac{3}{2} F_{1,2}^n(t), \quad F_3^V(t) = D_3^V(t) = 0, \quad (4.7)$$

with $t \equiv q^2$. At $t = 0$ we have

$$F_1^V(0) = 1, \quad D_1^V(0) = 0, \quad F_2^V(0) = \kappa_p + \frac{1}{2} \kappa_n, \quad D_2^V(0) = -\frac{3}{2} \kappa_n, \quad (4.8)$$

where $\kappa_p = 1.79$ and $\kappa_n = -1.91$ are the anomalous magnetic moments of the proton and neutron, respectively.

The experimental data are customarily described in terms of the electric and magnetic Sachs form factors $G_E^N(t)$ and $G_M^N(t)$ which are related to F_1^N and F_2^N via

$$G_E^{p,n}(t) = F_1^{p,n}(t) + \frac{t}{4m_N^2} F_2^{p,n}(t), \quad G_M^{p,n}(t) = F_1^{p,n}(t) + F_2^{p,n}(t). \quad (4.9)$$

A recent phenomenological fit to the experimental data of nucleon form factors has been carried out in [20] using the following parametrization:

$$\begin{aligned}
|G_M^p(t)| &= \left(\frac{x_1}{t^2} + \frac{x_2}{t^3} + \frac{x_3}{t^4} + \frac{x_4}{t^5} + \frac{x_5}{t^6} \right) \left[\ln \frac{t}{Q_0^2} \right]^{-\gamma}, \\
|G_M^n(t)| &= \left(\frac{y_1}{t^2} + \frac{y_2}{t^3} \right) \left[\ln \frac{t}{Q_0^2} \right]^{-\gamma},
\end{aligned} \tag{4.10}$$

where $Q_0 = \Lambda_{\text{QCD}} \approx 300$ MeV and $\gamma = 2 + \frac{4}{3\beta} = 2.148$. We will follow [20] to use the best fit values

$$\begin{aligned}
x_1 &= 429.88 \text{ GeV}^4, & x_2 &= -10783.69 \text{ GeV}^6, & x_3 &= 109738.41 \text{ GeV}^8, \\
x_4 &= -448583.96 \text{ GeV}^{10}, & x_5 &= 635695.29 \text{ GeV}^{12},
\end{aligned} \tag{4.11}$$

and

$$y_1 = 236.69 \text{ GeV}^4, \quad y_2 = -579.51 \text{ GeV}^6, \tag{4.12}$$

extracted from neutron data under the assumption $|G_E^n| = |G_M^n|$. Note that the form factors given by Eq. (4.10) do satisfy the constraint from perturbative QCD in the limit of large t [20]. Also as stressed in [20], time-like magnetic form factors are expected to behave like space-like magnetic form factors, i.e. real and positive for the proton, but negative for the neutron.

A new empirical fit to the reanalyzed data for $G_M^p(t)$ in the region $0 < t < 30 \text{ GeV}^2$ is recently given in [37]:

$$G_M^p(Q^2) = \frac{\mu_p}{1 + z_1 Q + z_2 Q^2 + z_3 Q^3 + z_4 Q^4 + z_5 Q^5}, \tag{4.13}$$

with

$$\begin{aligned}
z_1 &= (0.116 \pm 0.040) \text{ GeV}^{-1}, & z_2 &= (2.874 \pm 0.098) \text{ GeV}^{-2}, & z_3 &= (0.241 \pm 0.107) \text{ GeV}^{-3}, \\
z_4 &= (1.006 \pm 0.069) \text{ GeV}^{-4}, & z_5 &= (0.345 \pm 0.017) \text{ GeV}^{-5},
\end{aligned} \tag{4.14}$$

and $\mu_p = 2.79$. An empirical fit to the proton electromagnetic form factor ratio is also presented in [37]

$$\mu_p \frac{G_E^p(t)}{G_M^p(t)} = 1.0 - (0.130 \pm 0.005)[t - (0.04 \pm 0.09)], \tag{4.15}$$

for the range $0.04 < t < 5.6 \text{ GeV}^2$, indicating that the form factor ratio decreases with increasing Q^2 .

As for the axial form factors, no useful information can be extracted from SU(3) symmetry. Nevertheless, perturbative QCD indicates that, in the range of high Q^2 , the form factors $f_1(t)$ and $g_1(t)$ dominate at $t \rightarrow \infty$ and all others are suppressed by powers of m/Q [38]. Moreover, all octet-octet and octet-decuplet form factors at large t can be related to the magnetic form factors of the nucleon G_M^p and G_M^n (see Tables II-IV of [38]). Hence, the axial form factor g_1 at large momentum transfer is fixed.

A. Tree-dominated three-body decays

$$1. \quad \overline{B}^0 \rightarrow n\bar{p}\pi^+(\rho^+)$$

This decay receives factorizable contributions from Figs. 2(b), 2(d) with $b \rightarrow d$ penguin transition, 2(g) and a nonfactorizable contribution from Fig. 2(e). As the two-body baryonic decay, we can neglect the W -exchange contribution. Moreover, we shall assume that this mode is dominated by the factorizable term from Fig. 2(b) as it is governed by the parameter a_1 :

$$\mathcal{A}(\overline{B}^0 \rightarrow n\bar{p}\pi^+(\rho^+))_{\text{fact}} = \frac{G_F}{\sqrt{2}} V_{ud} V_{ub}^* a_1 \langle \pi^+(\rho^+) | (\bar{u}b)_{V-A} | \overline{B}^0 \rangle \langle n\bar{p} | (\bar{d}u)_{V-A} | 0 \rangle, \quad (4.16)$$

where $a_1 = c_1^{\text{eff}} + c_2^{\text{eff}}/3$ and we have neglected penguin contributions because the penguin Wilson coefficients c_3, \dots, c_{10} are numerically very small. The two-body meson matrix elements are parametrized in terms of the form factors F_0 and F_1 for $B - \pi$ transition

$$\langle \pi^+(p_\pi) | (\bar{u}b)_{V-A} | \overline{B}^0(p_B) \rangle = F_1^{B\pi}(q^2) (p_B + p_\pi)_\mu + \left(F_0^{B\pi}(q^2) - F_1^{B\pi}(q^2) \right) \frac{m_B^2 - m_\pi^2}{q^2} q_\mu, \quad (4.17)$$

and form factors V, A_0, A_1, A_2 for $B - \rho$ transition

$$\begin{aligned} \langle \rho^+(p_\rho) | (\bar{u}b)_{V-A} | \overline{B}^0(p_B) \rangle &= \frac{2}{m_B + m_\rho} \epsilon_{\mu\nu\alpha\beta} \varepsilon^{*\nu} p_B^\alpha p_\rho^\beta V^{B\rho}(q^2) - i \left\{ (m_B + m_\rho) \varepsilon_\mu^* A_1^{B\rho}(q^2) \right. \\ &\quad \left. - \frac{\varepsilon^* \cdot p_B}{m_B + m_\rho} (p_B + p_\rho)_\mu A_2^{B\rho}(q^2) - 2m_\rho \frac{\varepsilon^* \cdot p_B}{q^2} q_\mu [A_3^{B\rho}(q^2) - A_0^{B\rho}(q^2)] \right\}, \end{aligned} \quad (4.18)$$

with $q = p_B - p_{\pi(\rho)}$ and

$$A_3^{B\rho}(q^2) = \frac{m_B + m_\rho}{2m_\rho} A_1^{B\rho}(q^2) - \frac{m_B - m_\rho}{2m_\rho} A_2^{B\rho}(q^2). \quad (4.19)$$

The factorizable amplitude for the pion emission reads

$$\mathcal{A}(\overline{B}^0 \rightarrow n\bar{p}\pi^+)_{\text{fact}} = \frac{G_F}{\sqrt{2}} V_{ud} V_{ub}^* a_1 \bar{u}_n [(a\bar{p}_\pi + b) - (c\bar{p}_\pi + d)\gamma_5] v_{\bar{p}}, \quad (4.20)$$

where

$$\begin{aligned} a &= 2f_1^{np}(t)F_1^{B\pi}(t) + 4f_2^{np}(t)F_1^{B\pi}(t), \\ b &= -2f_2^{np}(t)F_1^{B\pi}(t)(p_n - p_{\bar{p}}) \cdot p_\pi / (2m_N) + f_3^{np}(t)F_0^{B\pi}(t)(m_B^2 - m_\pi^2) / (2m_N), \\ c &= 2g_1^{np}(t)F_1^{B\pi}(t), \\ d &= 2m_N g_1^{np}(t) \left[F_1^{B\pi}(t) + (F_0^{B\pi}(t) - F_1^{B\pi}(t)) \frac{m_B^2 - m_\pi^2}{t} \right] \\ &\quad - 2g_2^{np}(t)F_1^{B\pi}(t)(p_n - p_{\bar{p}}) \cdot p_\pi / (2m_N) + g_3^{np}(t)F_0^{B\pi}(t)(m_B^2 - m_\pi^2) / (2m_N), \end{aligned} \quad (4.21)$$

and $t \equiv q^2 = (p_B - p_\pi)^2 = (p_n + p_{\bar{p}})^2$. The amplitude for the ρ meson case is more cumbersome.

Since the relevant Clebsch-Gordon coefficients are $d^{np} = f^{np} = 1$, it follows from Eqs. (4.5) and (4.7) that the weak form factors have the form

$$f_{1,2}^{np}(t) = F_{1,2}^V(t) + D_{1,2}^V(t) = F_{1,2}^p(t) - F_{1,2}^n(t). \quad (4.22)$$

In terms of the nucleon magnetic and electric form factors, the weak form factors read

$$\begin{aligned} f_1^{np}(t) &= \frac{\frac{t}{4m_N^2}G_M^p(t) - G_E^p(t)}{t/(4m_N^2) - 1} - \frac{\frac{t}{4m_N^2}G_M^n(t) - G_E^n(t)}{t/(4m_N^2) - 1}, \\ f_2^{np}(t) &= -\frac{G_M^p(t) - G_E^p(t)}{t/(4m_N^2) - 1} + \frac{G_M^n(t) - G_E^n(t)}{t/(4m_N^2) - 1}. \end{aligned} \quad (4.23)$$

According to perturbative QCD, the weak form factors in the large t limit have the expressions [38]

$$f_1^{np}(t) \rightarrow G_M^p(t) - G_M^n(t), \quad g_1^{np}(t) \rightarrow \frac{5}{3}G_M^p(t) + G_M^n(t). \quad (4.24)$$

It is easily seen that this is consistent with the large t behavior of f_1^{np} given by Eq. (4.23).

The total decay rate for the process $\bar{B}^0(p_B) \rightarrow n(p_1) + \bar{p}(p_2) + \pi^+(p_3)$ is computed by

$$\Gamma = \frac{1}{(2\pi)^3} \frac{1}{32m_B^3} \int |\mathcal{A}|^2 dm_{12}^2 dm_{23}^2, \quad (4.25)$$

where $m_{ij}^2 = (p_i + p_j)^2$ with $p_3 = p_\pi$. To make a numerical estimate, we apply two different empirical fits of $G_M^p(t)$: Eq. (4.10) denoted by CHT (Chua-Hou-Tsai) and Eq. (4.13) denoted by BKLH (Brash-Kozlov-Li-Huber). For the proton electric form factor, we shall follow [20] to assume $|G_E^p(t)| = |G_M^p(t)|$ for CHT form factors and Eq. (4.15) for BKLH form factors. That is, we assume that Eq. (4.15) is applicable also to the large t region. As for $B - \pi(\rho)$ form factors, we consider two distinct models: the Bauer-Stech-Wirbel (BSW) model [39] and the Melikhov-Stech (MS) model based on the constituent quark picture [41].^{**} The BSW model assumes a monopole behavior for all the form factors. However, this is not consistent with heavy quark symmetry for heavy-to-light transitions. For example, the form factors F_1, V, A_0, A_2 in the infinite quark mass limit should have the same q^2 dependence and they differ from F_0 and A_1 by an additional pole factor [42]. Nevertheless, we apply this model for comparison.

^{**}The QCD sum rule method based on the light-cone sum rule analysis [40] is also one of the popular form-factor models. However, we found that some divergence occurs in the phase space integration when applying this model.

Considering only the vector-current contribution to baryon matrix element, we obtain the results shown in the first entry of Table III. Our calculations are in agreement with [18] when the BSW model and CHT form factors are used. However, we see from Table III that the branching ratio for $\bar{B}^0 \rightarrow n\bar{p}\rho^+$ in the BSW model is slightly larger. This is ascribed to the monopole form factor q^2 dependence for all the $B - \rho$ form factors. If one changes the form factor momentum dependence from monopole to dipole form for A_1 and V (sometimes referred to as the BSWII model in the literature), the resulting branching ratios are very similar to that in the MS model.

TABLE III. Branching ratios of $\bar{B}^0 \rightarrow n\bar{p}\pi^+(\rho^+)$ in two different form-factor models for $B - \pi(\rho)$ transition. Two distinct empirical fits for the proton magnetic form factor given in Eqs. (4.10) and (4.13), denoted by CHT and BKLH respectively, are utilized. The neutron form factors are taken from (4.10) and (4.12). Branching ratios in the first entry are without contributions from the axial form factors $g_i^{np}(t)$ and those in the second entry take into account contributions from the asymptotic form factor $g_1^{np}(t)$ given by Eq. (4.24).

	G_M^p (CHT)		G_M^p (BKLH)	
	MS	BSW	MS	BSW
$\bar{B}^0 \rightarrow n\bar{p}\pi^+$	1.7×10^{-6}	1.8×10^{-6}	8.0×10^{-7}	8.5×10^{-7}
	1.7×10^{-6}	1.9×10^{-6}	1.1×10^{-6}	1.3×10^{-6}
$\bar{B}^0 \rightarrow n\bar{p}\rho^+$	3.3×10^{-6}	4.8×10^{-6}	4.2×10^{-6}	5.5×10^{-6}
	3.4×10^{-6}	4.9×10^{-6}	4.6×10^{-6}	5.9×10^{-6}

To estimate the contribution from the axial vector current, we might assume that $g_1(t)$ takes the asymptotic form $\frac{5}{3}G_M^p(t) + G_M^n(t)$ [see Eq. (4.24)]. It turns out that the contribution due to $g_1(t)$ is very small for the CHT form factor G_M^p but not negligible for G_M^p (BKLH). It is interesting to notice that the rate of $n\bar{p}\rho^+$ is larger than that of $n\bar{p}\pi^+$ by a factor of $2 \sim 3$ if the CHT parametrization for G_M^p is employed, whereas the ratio becomes as large as 5 for G_M^p (BKLH).

Since both B^0 and \bar{B}^0 can decay into $n\bar{p}\pi^+(\rho^+)$, experimentally one has to disentangle the “background” contribution from the $B^0 - \bar{B}^0$ mixing or to tag the B meson. Therefore, we will give an estimate of $\bar{B}^0 \rightarrow p\bar{n}\pi^-(\rho^-)$ next.

2. $\bar{B}^0 \rightarrow p\bar{n}\pi^-(\rho^-)$

This decay receives contributions from Figs. 2(a), 2(e) and 2(g). As the previous decay, we will assume that it is dominated by the factorizable contribution from Fig. 2(a). Unfortunately, as shown in Eq. (4.1), it involves a three-body matrix element that cannot be evaluated directly. Instead, we will evaluate the low-lying pole diagrams with the strong

process $\overline{B}^0 \rightarrow \{\Lambda_b^{(*)}, \Sigma_b^{0(*)}\} \bar{n}$ followed by the weak decays $\{\Lambda_b^{(*)}, \Sigma_b^{0(*)}\} \rightarrow \pi^- p$.^{††} Consider the $\frac{1}{2}^+$ intermediate poles. Applying factorization to $\Lambda_b \rightarrow \pi^- p$ yields the pole amplitude

$$\begin{aligned} \mathcal{A}(\overline{B}^0 \rightarrow p \bar{n} \pi^-) = & -\frac{G_F}{\sqrt{2}} V_{ud} V_{ub}^* g_{\Lambda_b \rightarrow \overline{B}^0 n} f_\pi a_1 \bar{u}_p \left\{ f_1^{\Lambda_b p}(m_\pi^2) [2p_\pi \cdot p_p + \not{p}_\pi(m_{\Lambda_b} - m_p)] \gamma_5 \right. \\ & \left. + g_1^{\Lambda_b p}(m_\pi^2) [2p_\pi \cdot p_p - \not{p}_\pi(m_{\Lambda_b} + m_p)] \right\} v_{\bar{n}} \times \frac{1}{(p_p + p_\pi)^2 - m_{\Lambda_b}^2} \\ & + (\Lambda_b \rightarrow \Sigma_b^0), \end{aligned} \quad (4.26)$$

where we have employed the heavy-light baryon form factors defined by

$$\begin{aligned} \langle p(p_p) | (\bar{u}b)_{V\pm A} | \Lambda_b(p_{\Lambda_b}) \rangle = & \bar{u}_p \left\{ f_1^{\Lambda_b p}(p_\pi^2) \gamma_\mu + i \frac{f_2^{\Lambda_b p}(p_\pi^2)}{m_{\Lambda_b} + m_p} \sigma_{\mu\nu} p_\pi^\nu + \frac{f_3^{\Lambda_b p}(p_\pi^2)}{m_{\Lambda_b} + m_p} p_{\pi\mu} \right. \\ & \left. \pm \left[g_1^{\Lambda_b p}(p_\pi^2) \gamma_\mu + i \frac{g_2^{\Lambda_b p}(p_\pi^2)}{m_{\Lambda_b} + m_p} \sigma_{\mu\nu} p_\pi^\nu + \frac{g_3^{\Lambda_b p}(p_\pi^2)}{m_{\Lambda_b} + m_p} p_{\pi\mu} \right] \gamma_5 \right\} u_{\Lambda_b}, \end{aligned} \quad (4.27)$$

with $p_\pi = p_{\Lambda_b} - p_p$.

For the heavy-light form factors $f_i^{\mathcal{B}_1 \mathcal{B}_2}$ and $g_i^{\mathcal{B}_1 \mathcal{B}_2}$, we will follow [43] to apply the non-relativistic quark model to evaluate the weak current-induced baryon form factors at zero recoil in the rest frame of the heavy parent baryon, where the quark model is most trustworthy. This quark model approach has the merit that it is applicable to heavy-to-heavy and heavy-to-light baryonic transitions at maximum q^2 . Following [44] we have^{‡‡}

$$\begin{aligned} f_1^{\Lambda_b p}(q_m^2) = g_1^{\Lambda_b p}(q_m^2) &= 0.86, \quad f_2^{\Lambda_b p}(q_m^2) = g_3^{\Lambda_b p}(q_m^2) = -0.51, \\ f_3^{\Lambda_b p}(q_m^2) = g_2^{\Lambda_b p}(q_m^2) &= -0.22, \end{aligned} \quad (4.28)$$

for $\Lambda_b - p$ transition at zero recoil $q_m^2 = (m_{\Lambda_b} - m_p)^2$, and

$$\begin{aligned} f_1^{\Sigma_b^0 p}(q_m^2) &= 1.65, \quad f_2^{\Sigma_b^0 p}(q_m^2) = 1.92, \quad f_3^{\Sigma_b^0 p}(q_m^2) = -1.72, \\ g_1^{\Sigma_b^0 p}(q_m^2) &= -0.17, \quad g_2^{\Sigma_b^0 p}(q_m^2) = 0.04, \quad g_3^{\Sigma_b^0 p}(q_m^2) = 0.10, \end{aligned} \quad (4.29)$$

for $\Sigma_b^0 - p$ transition at $q_m^2 = (m_{\Sigma_b} - m_p)^2$. Since the calculation for the q^2 dependence of form factors is beyond the scope of the non-relativistic quark model, we will follow the conventional practice to assume a pole dominance for the form-factor q^2 behavior:

^{††}There is another pole diagram with the weak decay $\overline{B}^0 \rightarrow \pi^- \pi^+(\rho^+)$ followed by the strong process $\pi^+(\rho^+) \rightarrow p \bar{n}$ [see Fig. 2(a)]. However, this pole amplitude is expected to be suppressed as the intermediate pion state is far off its mass shell. Consequently, the nucleon-nucleon-pion coupling is subject to a large suppression due to the form-factor effects at large q^2 .

^{‡‡}The form factors for $\Lambda_b - p$ transition at $q^2 = 0$ are given in Table I of [44]. For $\Sigma_b^0 - p$ form factors at zero recoil, it can be evaluated using Eq. (22) of [43]. Note that the spin factor is $\eta = -\frac{1}{3}$ and the flavor factor is $N_{\Sigma_b^0 p} = 1/\sqrt{6}$ for $\Sigma_b^0 - p$ transition.

$$f(q^2) = f(q_m^2) \left(\frac{1 - q_m^2/m_V^2}{1 - q^2/m_V^2} \right)^n, \quad g(q^2) = g(q_m^2) \left(\frac{1 - q_m^2/m_A^2}{1 - q^2/m_A^2} \right)^n, \quad (4.30)$$

where m_V (m_A) is the pole mass of the vector (axial-vector) meson with the same quantum number as the current under consideration. The function

$$G(q^2) = \left(\frac{1 - q_m^2/m_{\text{pole}}^2}{1 - q^2/m_{\text{pole}}^2} \right)^n \quad (4.31)$$

plays the role of the baryon Isgur-Wise function $\zeta(\omega)$ for $\Lambda_Q \rightarrow \Lambda_{Q'}$ transition, namely, $G = 1$ at $q^2 = q_m^2$. Previous model calculations of $\zeta(\omega)$ [45–49] indicates that it is consistent with $G(q^2)$ with $n = 2$. However, a recent calculation of $\zeta(\omega)$ in [50] yields

$$\zeta(\omega) = \left(\frac{2}{1 + \omega} \right)^{1.23+0.4/\omega} \quad (4.32)$$

and this clearly favors $n = 1$. As we shall below, the recent first observation of $B^- \rightarrow p\bar{p}K^-$ by Belle [23] also favors a monopole q^2 dependence for baryon form factors.

The calculation of $\bar{B}^0 \rightarrow p\bar{n}\rho^-$ is similar to that of $p\bar{n}\pi^-$ except that the vacuum- ρ matrix element now reads

$$\langle \rho^- | \bar{d}\gamma_\mu u | 0 \rangle = f_\rho m_\rho \varepsilon_\mu^*, \quad (4.33)$$

and that the computation is much more tedious than the pion case, though it is straightforward. Using the pole masses $m_V = 5.32$ GeV, $m_A = 5.71$ GeV and the decay constant $f_\rho = 216$ MeV, we obtain

$$\begin{aligned} \mathcal{B}(\bar{B}^0 \rightarrow p\bar{n}\pi^-) &= 2.8 \times 10^{-6} \quad (2.7 \times 10^{-7}), \\ \mathcal{B}(\bar{B}^0 \rightarrow p\bar{n}\rho^-) &= 8.2 \times 10^{-6} \quad (8.2 \times 10^{-7}), \end{aligned} \quad (4.34)$$

for a monopole (dipole) q^2 dependence for baryon form factors. Since $g_{\Lambda_b \rightarrow \bar{B}^0 n} = -3\sqrt{3} g_{\Sigma_b^0 \rightarrow \bar{B}^0 n}$ [cf. Eq. (3.20)], the contribution due to the Λ_b and Σ_b^0 poles is destructive. In the calculation we have used $|g_{\Lambda_b \rightarrow \bar{B}^0 n}| = 16$ [21].

Three remarks are in order. First, in the calculation we have neglected other nonfactorizable contributions from Fig. 2(e). For the pole diagrams, we did not evaluate the $\frac{1}{2}$ -pole contributions owing to the technical difficulties for the bag model in dealing with the negative-parity baryon states. Second, since $n = 1$ is favored by the recent measurement of the decay $B^- \rightarrow p\bar{p}K^-$, as we shall see below, it turns out that $B^0 \rightarrow n\bar{p}\rho^+$ has a large branching ratio of order 1×10^{-5} for $n = 1$. Third, the decay $\bar{B}^0 \rightarrow p\bar{n}\pi^-$ receives the resonant contribution $\bar{B}^0 \rightarrow p\bar{\Delta}^-$ followed by the strong decay $\bar{\Delta}^- \rightarrow \bar{n}\pi^-$. Since the branching ratio for $\bar{B}^0 \rightarrow p\bar{\Delta}^-$ is only of order 6×10^{-8} (see Table II), the resonant contribution due to the Δ is thus negligible.

$$3. \quad \underline{\bar{B}^0 \rightarrow \{\Sigma^0\bar{\Sigma}^-, \Sigma^-\bar{\Lambda}, \Xi^-\bar{\Xi}^0\}\pi^+(\rho^+)}$$

The calculation for the decays $\bar{B}^0 \rightarrow \{\Sigma^0 \bar{\Sigma}^-, \Sigma^- \bar{\Lambda}, \Xi^- \bar{\Xi}^0\} \pi^+(\rho^+)$ is the same as that for $\bar{B}^0 \rightarrow n \bar{p} \pi^+(\rho^+)$ except for different baryonic form factors in the final states. The relevant Clebsch-Gordon coefficients for weak form factors are (see e.g. [36])

$$\begin{aligned} d^{\Lambda \Sigma^+} &= \sqrt{\frac{2}{3}}, & d^{\Sigma^0 \Sigma^+} &= 0, & d^{\Xi^0 \Xi^+} &= 1, \\ f^{\Lambda \Sigma^+} &= 0, & f^{\Sigma^0 \Sigma^+} &= \sqrt{2}, & f^{\Xi^0 \Xi^+} &= -1. \end{aligned} \quad (4.35)$$

Then (4.5) and (4.7) lead to

$$\begin{aligned} f_{1,2}^{\Lambda \Sigma^+}(t) &= -\sqrt{\frac{3}{2}} F_{1,2}^n(t), & f_{1,2}^{\Xi^0 \Xi^+} &= -F_{1,2}^p(t) - 2F_{1,2}^n(t), \\ f_{1,2}^{\Sigma^0 \Sigma^+}(t) &= \sqrt{2} F_{1,2}^p(t) + \frac{1}{\sqrt{2}} F_{1,2}^n(t). \end{aligned} \quad (4.36)$$

A straightforward calculation gives $\mathcal{B}(\bar{B}^0 \rightarrow \Sigma^- \bar{\Lambda} \pi^+) = 2.9 \times 10^{-7}$, $\mathcal{B}(\bar{B}^0 \rightarrow \Xi^- \bar{\Xi}^0 \pi^+) = 2.0 \times 10^{-7}$ and $\mathcal{B}(\bar{B}^0 \rightarrow \Sigma^0 \bar{\Sigma}^- \pi^+) = 6.4 \times 10^{-9}$. Compared to the $n \bar{p} \pi^+$ mode, the decay rates of above three decays are suppressed owing to smaller baryon form factors and less three-body phase spaces available.

4. $B^- \rightarrow \{p \bar{p}, n \bar{n}, \Sigma^+ \bar{\Sigma}^-, \dots\} \pi^-(\rho^-)$

Let us first consider the decay $B^- \rightarrow p \bar{p} \pi^-$. It receives factorizable contributions from Figs. 2(a) and 2(d):

$$\begin{aligned} A(B^- \rightarrow p \bar{p} \pi^-)_{\text{fact}} &= \frac{G_F}{\sqrt{2}} V_{ub} V_{ud}^* \left\{ a_1 \langle \pi^- | (\bar{d}u)_{V-A} | 0 \rangle \langle p \bar{p} | (\bar{u}b)_{V-A} | B^- \rangle \right. \\ &\quad \left. + a_2 \langle \pi^- | (\bar{d}b)_{V-A} | B^- \rangle \langle p \bar{p} | (\bar{u}u)_{V-A} | 0 \rangle \right\} \equiv A_1 + A_2, \end{aligned} \quad (4.37)$$

where $a_{1,2} = c_{1,2}^{\text{eff}} + c_{2,1}^{\text{eff}}/3$. In analog to the previous mode, we will evaluate the corresponding low-lying pole diagrams for the factorizable external W -emission amplitude, namely, the strong process $B^- \rightarrow \{\Lambda_b^{(*)}, \Sigma_b^{0(*)}\} \bar{p}$, followed by the weak decay $\{\Lambda_b^{(*)}, \Sigma_b^{0(*)}\} \rightarrow p \pi^-$. Its amplitude governed by the $\frac{1}{2}^+$ poles is given by

$$\begin{aligned} A_1 &= -\frac{G_F}{\sqrt{2}} V_{ub} V_{ud}^* g_{\Lambda_b \rightarrow B^- p} f_\pi a_1 \bar{u}_p \left\{ f_1^{\Lambda_b p}(m_\pi^2) [2p_\pi \cdot p_p + \not{p}_\pi(m_{\Lambda_b} - m_p)] \gamma_5 \right. \\ &\quad \left. + g_1^{\Lambda_b p}(m_\pi^2) [2p_\pi \cdot p_p - \not{p}_\pi(m_{\Lambda_b} + m_p)] \right\} v_{\bar{p}} \times \frac{1}{(p_p + p_\pi)^2 - m_{\Lambda_b}^2} \\ &\quad + (\Lambda_b \rightarrow \Sigma_b^0), \end{aligned} \quad (4.38)$$

where we have applied factorization to the weak decay $\{\Lambda_b, \Sigma_b^0\} \rightarrow p \pi^-$. To evaluate the factorizable amplitude A_2 , we apply the isospin symmetry relations^{§§}

§§This isospin relation amounts to assuming $\langle N | (\bar{s}s)_{V-A} | N \rangle = 0$, an assumption supported by the OZI rule.

$$\langle n | (\bar{u}u)_{V-A} | n \rangle = \langle p | (\bar{d}d)_{V-A} | p \rangle, \quad \langle n | (\bar{d}d)_{V-A} | n \rangle = \langle p | (\bar{u}u)_{V-A} | p \rangle, \quad (4.39)$$

to relate the form factors f_1^{pp} and f_2^{pp} appearing in the vector current $p\bar{p}$ matrix element

$$\langle p(p_1)\bar{p}(p_2) | \bar{u}\gamma_\mu u | 0 \rangle = \bar{u}_p(p_1) \left[f_1^{pp}(q^2) \gamma_\mu + i \frac{f_2^{pp}(q^2)}{2m_p} \sigma_{\mu\nu} q^\nu \right] v_{\bar{p}}(p_2), \quad (4.40)$$

to the electromagnetic form factors F_1 and F_2 defined in the nucleon matrix element Eq. (4.6). We find

$$f_1^{pp}(t) = 2F_1^p(t) + F_1^n(t), \quad f_2^{pp}(t) = 2F_2^p(t) + F_2^n(t). \quad (4.41)$$

A straightforward calculation indicates that the contribution from a_2 is small and negligible due mainly to the small vector form factors $f_{1,2}^{pp}$. The a_1 contribution gives a branching ratio of order 3.8×10^{-6} for $n = 1$ and 2.7×10^{-7} for $n = 2$. As we shall see below, as far as the factorizable a_1 contribution is concerned, the tree-dominated $B^- \rightarrow p\bar{p}\pi^-$ and the penguin-dominated decay $B^- \rightarrow p\bar{p}K^-$ have almost the same rate and the latter has been observed recently [23]. In some sense this is very similar to the mesonic decays $B \rightarrow K\pi$ and $\pi\pi$. Without the chiral enhancement for penguin contributions, one will have $\pi\pi > K\pi$. The experimental observation [51] that $K^-\pi^+ > \pi^-\pi^+$ and $\bar{K}^0\pi^- > \pi^0\pi^-$ clearly implies the importance of penguin chiral enhancement. It is quite possible that for baryonic B decay we also have $p\bar{p}K^- > p\bar{p}\pi^-$. Note that the a_2 contribution to $p\bar{p}\pi^-$ is destructive and it is subject to many uncertainties. For example, the axial-vector current contribution to the $p\bar{p}$ matrix element has been neglected so far and the value of a_2 is numerically very small if $a_2 = c_2^{\text{eff}} + c_1^{\text{eff}}/3$. A large value of a_2 of order 0.40–0.55 [52], as indicated by the recent observation of $\bar{B}^0 \rightarrow D^0\pi^0$ [53], and an inclusion of axial form factor contributions may suppress $p\bar{p}\pi^-$ relative to $p\bar{p}K^-$. Another effect we have neglected thus far is the penguin contribution. Just as the $B \rightarrow \pi\pi$ decay, the tree-penguin interference for $B^- \rightarrow p\bar{p}\pi^-$ may turn out to be destructive for a certain range of the phase angle γ . In view of the aforementioned considerations, we will prefer to carry out a full analysis of $B^- \rightarrow \{p\bar{p}, n\bar{n}, \Sigma^+\bar{\Sigma}^-, \dots\} \pi^-(\rho^-)$ decays in a separate publication. It appears to us that $B^- \rightarrow p\bar{p}\pi^-$ should have a branching ratio at least of order 10^{-6} , based on the recent measurement of $B^- \rightarrow p\bar{p}K^-$ to be discussed below.

Thus far we have focused on the nonresonant decay of $p\bar{p}\pi^-$. It also receives resonant contributions, for example $B^- \rightarrow p\bar{\Delta}^{--}$ and $B^- \rightarrow \bar{p}N^0(1440)$. As discussed in Sec. III.A, the branching ratio of the former is of order $(1-2) \times 10^{-6}$, to be compared with the recent measurement by Belle [23]

$$\mathcal{B}(B^- \rightarrow p\bar{p}\pi^-) = (1.9_{-0.9}^{+1.0} \pm 0.3) \times 10^{-6}. \quad (4.42)$$

Therefore, the direct nonresonant contribution is probably smaller than the resonant ones. Experimentally, it is thus important to study the resonance effects through the Dalitz plot analysis.

B. Penguin-dominated three-body decays

1. $\overline{B} \rightarrow N\overline{N}K^{(*)}$

The decay $B^- \rightarrow p\bar{p}K^{(*)}$ is mainly governed by the diagrams Figs. 2(a) and 2(c) with the factorizable amplitude

$$\begin{aligned} \mathcal{A}(B^- \rightarrow p\bar{p}K^{(*)})_{\text{fact}} = & \frac{G_F}{\sqrt{2}} \left\{ V_{ub}V_{us}^* \left[a_1 \langle K^{(*)} | (\bar{s}u)_{V-A} | 0 \rangle \langle p\bar{p} | (\bar{u}b)_{V-A} | B^- \rangle \right. \right. \\ & + a_2 \langle p\bar{p} | (\bar{u}u)_{V-A} | 0 \rangle \langle K^{(*)} | (\bar{s}b)_{V-A} | B^- \rangle \\ & - V_{tb}V_{ts}^* \left[a_3 \langle p\bar{p} | (\bar{u}u + \bar{d}d + \bar{s}s)_{V-A} | 0 \rangle \langle K^{(*)} | (\bar{s}b)_{V-A} | B^- \rangle \right. \\ & + a_5 \langle p\bar{p} | (\bar{u}u + \bar{d}d + \bar{s}s)_{V+A} | 0 \rangle \langle K^{(*)} | (\bar{s}b)_{V-A} | B^- \rangle \\ & + (a_4 + a_{10}) \langle K^{(*)} | (\bar{s}u)_{V-A} | 0 \rangle \langle p\bar{p} | (\bar{u}b)_{V-A} | B^- \rangle \\ & - 2(a_6 + a_8) \langle K^{(*)} | \bar{s}(1 + \gamma_5)u | \bar{0} \rangle \langle p\bar{p} | \bar{u}(1 - \gamma_5)b | B^- \rangle \quad (4.43) \\ & + (a_4 + a_{10}) \langle K^{(*)} p\bar{p} | (\bar{s}u)_{V-A} | 0 \rangle \langle 0 | (\bar{u}b)_{V-A} | B^- \rangle \\ & - 2(a_6 + a_8) \langle K^{(*)} p\bar{p} | \bar{s}(1 + \gamma_5)u | 0 \rangle \langle 0 | \bar{u}(1 - \gamma_5)b | B^- \rangle \\ & \left. \left. + a_9 \langle p\bar{p} | (\bar{u}u - \frac{1}{3}\bar{d}d - \frac{1}{3}\bar{s}s)_{V+A} | 0 \rangle \langle K^{(*)} | (\bar{s}b)_{V-A} | B^- \rangle \right] \right\}, \end{aligned}$$

with

$$a_{2i} = c_{2i}^{\text{eff}} + \frac{1}{N_c} c_{2i-1}^{\text{eff}}, \quad a_{2i-1} = c_{2i-1}^{\text{eff}} + \frac{1}{N_c} c_{2i}^{\text{eff}}. \quad (4.44)$$

In Eq. (4.43) the last two terms correspond to weak annihilation. As in the decay $\overline{B}^0 \rightarrow p\bar{n}\pi^-$, since we do not know how to evaluate the 3-body hadronic matrix element, we will instead evaluate the corresponding low-lying pole diagrams with the strong process $B^- \rightarrow \{\Lambda_b^{(*)}, \Sigma_b^{0(*)}\}\bar{p}$ followed by the weak decays $\{\Lambda_b^{(*)}, \Sigma_b^{0(*)}\} \rightarrow K^{(*)}p$ [cf. Figs. 2(a) and 2(c)]. Consider the $\frac{1}{2}^+$ intermediate poles and the final state K^- first. Applying factorization to $\Lambda_b \rightarrow K^-p$ yields

$$\begin{aligned} \langle K^- p | \mathcal{H}_W | \Lambda_b \rangle = & \frac{G_F}{\sqrt{2}} \left\{ \left[V_{ub}V_{us}^* a_1 - V_{tb}V_{ts}^* (a_4 + a_{10}) \right] \langle K^- | (\bar{s}u)_{V-A} | 0 \rangle \langle p | (\bar{u}b)_{V-A} | \Lambda_b \rangle \right. \\ & \left. + 2V_{tb}V_{ts}^* (a_6 + a_8) \frac{m_K^2}{m_b m_s} \langle K^- | (\bar{s}u)_{V+A} | 0 \rangle \langle p | (\bar{u}b)_{V+A} | \Lambda_b \rangle \right\}, \quad (4.45) \end{aligned}$$

where we have applied equations of motion

$$-i\partial^\mu(\bar{q}_1\gamma_\mu q_2) = (m_1 - m_2)\bar{q}_1q_2, \quad -i\partial^\mu(\bar{q}_1\gamma_\mu\gamma_5 q_2) = (m_1 + m_2)\bar{q}_1\gamma_5q_2. \quad (4.46)$$

The pole amplitude then has the form

$$\begin{aligned}
\mathcal{A}(B^- \rightarrow p\bar{p}K^-) = & -\frac{G_F}{\sqrt{2}} g_{\Lambda_b^0 \rightarrow B^- p} f_K \bar{u}_p \left\{ f_1^{\Lambda_b p}(m_K^2) h \left[2p_K \cdot p_p + \not{p}_K (m_{\Lambda_b} - m_p) \right] \gamma_5 \right. \\
& \left. + g_1^{\Lambda_b p}(m_K^2) h' \left[2p_K \cdot p_p - \not{p}_K (m_{\Lambda_b} + m_p) \right] \right\} v_{\bar{p}} \times \frac{1}{(p_p + p_K)^2 - m_{\Lambda_b}^2} \\
& + (\Lambda_b \rightarrow \Sigma_b^0), \tag{4.47}
\end{aligned}$$

with

$$\begin{aligned}
h &= V_{ub} V_{us}^* a_1 - V_{tb} V_{ts}^* \left\{ a_4 + a_{10} + 2(a_6 + a_8) \frac{m_K^2}{m_b m_s} \right\}, \\
h' &= V_{ub} V_{us}^* a_1 - V_{tb} V_{ts}^* \left\{ a_4 + a_{10} - 2(a_6 + a_8) \frac{m_K^2}{m_b m_s} \right\}. \tag{4.48}
\end{aligned}$$

Since $g_{\Lambda_b \rightarrow B^- p} = 3\sqrt{3} g_{\Sigma_b^0 \rightarrow B^- p}$ [Eq. (3.23)], it is evident that the pole contributions arising from the Λ_b and Σ_b^0 intermediate states are constructive and dominated by the former one.

The amplitude of $B^- \rightarrow p\bar{p}K^{*-}$ is similar to that of $p\bar{p}K^-$ except that there are no a_6 and a_8 penguin contributions to h or h' given in Eq. (4.48) owing to the fact that $\langle K^{*-} | \bar{s}u | 0 \rangle = 0$. For numerical calculations of decay rates we use the running quark masses $m_b(m_b) = 4.4$ GeV, $m_s(m_b) = 90$ MeV and the decay constant $f_{K^*} = 221$ MeV. Note that the corresponding running strange quark mass at $\mu = 1$ GeV is 140 MeV. Applying the baryon form factors given by Eqs. (4.28) and (4.29) we obtain

$$\begin{aligned}
\mathcal{B}(B^- \rightarrow p\bar{p}K^-) &= 4.0 \times 10^{-6} \quad (2.3 \times 10^{-7}), \\
\mathcal{B}(B^- \rightarrow p\bar{p}K^{*-}) &= 2.3 \times 10^{-6} \quad (2.1 \times 10^{-7}), \tag{4.49}
\end{aligned}$$

for $n = 1$ ($n = 2$), where use of the strong coupling $|g_{\Lambda_b^0 \rightarrow B^- p}| = 16$ has been made. As stressed before, the large chiral enhancement of penguin contributions characterized by the $m_K^2/(m_b m_s)$ term accounts for the sizable decay rate of $B^- \rightarrow p\bar{p}K^-$.

An observation of this mode has recently been reported by Belle [23]

$$\mathcal{B}(B^- \rightarrow p\bar{p}K^-) = (4.3_{-0.9}^{+1.1} \pm 0.5) \times 10^{-6}. \tag{4.50}$$

This is the first ever measurement of the penguin-dominated charmless baryonic B decay. Evidently, the model prediction is in good agreement with experiment provided that the baryon form factor q^2 dependence is of the monopole form (i.e. $n = 1$). However, in view of many assumptions and uncertainties involved in the calculation, the statement about the monopole q^2 dependence for heavy-to-light baryonic form factors should be regarded as a suggestion rather than a firm one. The absence of penguin contributions of a_6 and a_8 to K^* production explains why the $p\bar{p}K^{*-}$ rate is smaller than $p\bar{p}K^-$, contrary to the case of $\bar{B}^0 \rightarrow n\bar{p}\pi^+(\rho^+)$ where the ratio of ρ^+/π^+ can be as large as 5.

In Fig. 3 we show the differential decay rate $d\Gamma/dt$ of $B^- \rightarrow p\bar{p}K^-$ where $t = (p_p + p_{\bar{p}})^2 = (p_B - p_K)^2$. Evidently, the spectrum peaks at $t \sim 5.5$ GeV 2 , indicating a threshold

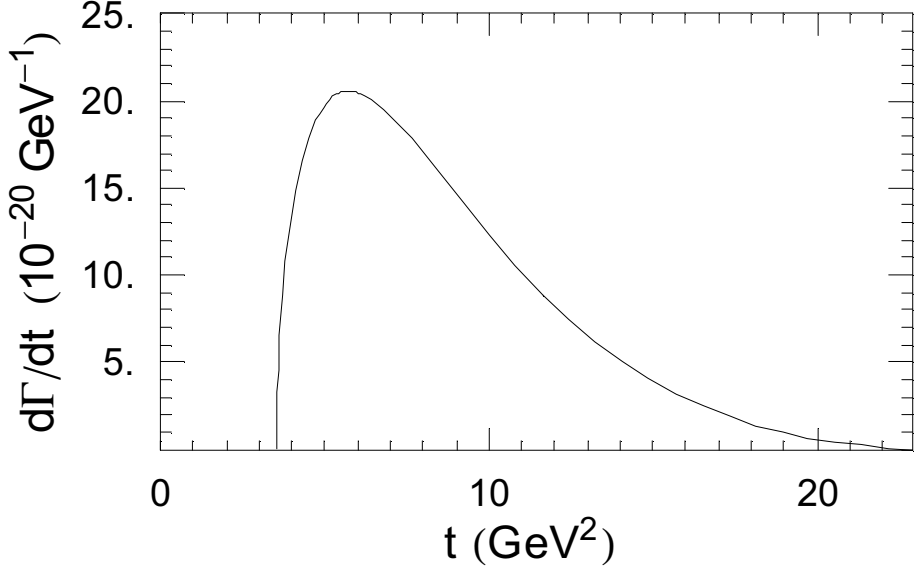


FIG. 3. The differential decay rate of $B^- \rightarrow p\bar{p}K^-$ where $t = (p_p + p_{\bar{p}})^2 = (p_B - p_K)^2$.

enhancement for baryon production and a fast recoil kaon accompanied by a baryon pair with low invariant mass.

For other $N\bar{N}K^{(*)}$ modes, it is easily seen that the pole amplitude of $\bar{B}^0 \rightarrow p\bar{n}K^{(*)}$ is very similar to that of $B^- \rightarrow p\bar{p}K^{(*)}$ except the Λ_b and Σ_b^0 poles contribute destructively owing to the relation $g_{\Lambda_b \rightarrow \bar{B}^0 n} = -3\sqrt{3}g_{\Sigma_b^0 \rightarrow \bar{B}^0 n}$ [Eq. (3.20)]. Repeating the same calculation as before gives

$$\begin{aligned} \mathcal{B}(\bar{B}^0 \rightarrow p\bar{n}K^-) &= 1.9 \times 10^{-6} \quad (1.5 \times 10^{-7}), \\ \mathcal{B}(\bar{B}^0 \rightarrow p\bar{n}K^{*-}) &= 1.8 \times 10^{-6} \quad (1.9 \times 10^{-7}), \end{aligned} \quad (4.51)$$

for $n = 1$ ($n = 2$). As for $\bar{B}^0 \rightarrow n\bar{n}\bar{K}^{0(*)}$, its pole amplitude is the same as $\bar{B}^0 \rightarrow p\bar{n}K^{(*)}$ except that the electroweak parameters a_8 and a_{10} in Eq. (4.48) are replaced by $-\frac{1}{2}a_8$ and $-\frac{1}{2}a_{10}$, respectively. Since these parameters are very small, the mode $n\bar{n}\bar{K}^{0(*)}$ has a similar rate as $p\bar{n}K^{(*)}$.

As for the decays $\bar{B}^0 \rightarrow p\bar{p}\bar{K}^{0(*)}$ and $B^- \rightarrow n\bar{n}K^{(*)}$, their branching ratios are suppressed, of order a few times of 10^{-7} for K production and 5×10^{-8} for K^* . This is attributed to the fact that only the Σ_b pole contributes and its coupling with the B meson and the nucleon is smaller compared to Λ_b . The current limit is $\mathcal{B}(\bar{B}^0 \rightarrow p\bar{p}\bar{K}^0) < 7.2 \times 10^{-6}$ [23].

2. $\bar{B}^0 \rightarrow \Lambda\bar{p}\pi^+(\rho^+)$

This decay receives contributions from Figs. 2(b), 2(d), 2(e) and 2(g). The factorizable amplitude from Figs. (2b) and 2(d) including tree and penguin transitions is

$$\begin{aligned}
\mathcal{A}(\bar{B}^0 \rightarrow \Lambda \bar{p} \pi^+(\rho^+))_{\text{fact}} = & \frac{G_F}{\sqrt{2}} \left\{ V_{ub} V_{us}^* a_1 \langle \pi^+(\rho^+) | (\bar{u}b)_{V-A} | \bar{B}^0 \rangle \langle \Lambda \bar{p} | (\bar{s}u)_{V-A} | 0 \rangle \right. \\
& - V_{tb} V_{ts}^* \left[(a_4 + a_{10}) \langle \pi^+(\rho^+) | (\bar{u}b)_{V-A} | \bar{B}^0 \rangle \langle \Lambda \bar{p} | (\bar{s}u)_{V-A} | 0 \rangle \right. \quad (4.52) \\
& - 2(a_6 + a_8) \langle \pi^+(\rho^+) | \bar{u}(1 - \gamma_5)b | \bar{B}^0 \rangle \langle \Lambda \bar{p} | \bar{s}(1 + \gamma_5)u | 0 \rangle \\
& + (a_4 - \frac{1}{2}a_{10}) \langle \pi^+(\rho^+) \Lambda \bar{p} | (\bar{s}d)_{V-A} | 0 \rangle \langle 0 | (\bar{d}b)_{V-A} | \bar{B}^0 \rangle \\
& \left. \left. - 2(a_6 - \frac{1}{2}a_8) \langle \pi^+(\rho^+) \Lambda \bar{p} | \bar{s}(1 + \gamma_5)d | 0 \rangle \langle 0 | \bar{d}(1 - \gamma_5)b | \bar{B}^0 \rangle \right] \right\},
\end{aligned}$$

where the first term corresponds to external W -emission, second and third terms to the $b \rightarrow s$ penguin transition and the last two terms to penguin-induced weak annihilation. We shall neglect the weak-annihilation contributions in the practical calculation. Applying equations of motion we obtain

$$\begin{aligned}
\langle \Lambda \bar{p} | \bar{s}(1 + \gamma_5)u | 0 \rangle = & \frac{(p_\Lambda + p_{\bar{p}})^\mu}{m_s - m_\mu} \langle \Lambda \bar{p} | \bar{s} \gamma_\mu b | 0 \rangle + \frac{(p_\Lambda + p_{\bar{p}})^\mu}{m_s + m_\mu} \langle \Lambda \bar{p} | \bar{s} \gamma_\mu \gamma_5 b | 0 \rangle \\
= & \frac{m_\Lambda - m_p}{m_s - m_u} f_1^{\Lambda p}(t) \bar{u}_\Lambda v_{\bar{p}} + \frac{1}{m_s + m_u} \left[(m_\Lambda + m_p) g_1^{\Lambda p}(t) \right. \\
& \left. + \frac{t}{m_\Lambda + m_p} g_3^{\Lambda p}(t) \right] \bar{u}_\Lambda \gamma_5 v_{\bar{p}}, \quad (4.53)
\end{aligned}$$

where $t = (p_\Lambda + p_{\bar{p}})^2$ and we have taken the SU(3) symmetry result $f_3^{\Lambda p}(t) = 0$ [see Eqs. (4.5) and (4.7)]. Since the pseudoscalar form factor g_3 corresponds to a kaon pole contribution to the $\Lambda \bar{p}$ axial matrix element, it follows that

$$g_3^{\Lambda p}(t) = -\frac{(m_\Lambda + m_p)^2}{t - m_K^2} g_1^{\Lambda p}(t). \quad (4.54)$$

Consequently,

$$\langle \Lambda \bar{p} | \bar{s}(1 + \gamma_5)u | 0 \rangle = \frac{m_\Lambda - m_p}{m_s - m_u} f_1^{\Lambda p}(t) \bar{u}_\Lambda v_{\bar{p}} - \frac{m_\Lambda + m_p}{m_s + m_u} \frac{m_K^2}{t - m_K^2} g_1^{\Lambda p}(t) \bar{u}_\Lambda \gamma_5 v_{\bar{p}}. \quad (4.55)$$

It is easily seen that the first term on the right hand side satisfies the relation of vector current conservation in the SU(3) limit, while the second term respects the PCAC relation. Therefore, the above expression has a smooth chiral behavior in the zero light quark mass limit $m_s, m_u \rightarrow 0$. Applying equations of motion again yields

$$\begin{aligned}
\langle \pi^+ | \bar{u}(1 - \gamma_5)b | \bar{B}^0 \rangle &= \frac{m_B^2 - m_\pi^2}{m_b} F_0^{B\pi}(t), \\
\langle \rho^+ | \bar{u}(1 - \gamma_5)b | \bar{B}^0 \rangle &= 2i \frac{m_\rho}{m_b} A_0^{B\rho}(t) (\varepsilon^* \cdot p_B), \quad (4.56)
\end{aligned}$$

where use of Eqs. (4.17-4.19) has been made. Therefore, the third term in Eq. (4.52) is reduced to

$$\begin{aligned}
\langle \pi^+ | \bar{u}(1 - \gamma_5)b | \bar{B}^0 \rangle \langle \Lambda \bar{p} | \bar{s}(1 + \gamma_5)u | 0 \rangle &= \frac{m_B^2 - m_\pi^2}{m_b} F_0^{B\pi}(t) \bar{u}_\Lambda \left[\frac{m_\Lambda - m_p}{m_s - m_u} f_1^{\Lambda p}(t) \right. \\
&\quad \left. - \frac{m_\Lambda + m_p}{m_s + m_u} \frac{m_K^2}{t - m_K^2} g_1^{\Lambda p}(t) \gamma_5 \right] v_{\bar{p}}, \\
\langle \rho^+ | \bar{u}(1 - \gamma_5)b | \bar{B}^0 \rangle \langle \Lambda \bar{p} | \bar{s}(1 + \gamma_5)u | 0 \rangle &= 2i \frac{m_\rho}{m_b} A_0^{B\rho}(t) (\varepsilon^* \cdot p_B) \bar{u}_\Lambda \left[\frac{m_\Lambda - m_p}{m_s - m_u} f_1^{\Lambda p}(t) \right. \\
&\quad \left. - \frac{m_\Lambda + m_p}{m_s + m_u} \frac{m_K^2}{t - m_K^2} g_1^{\Lambda p}(t) \gamma_5 \right] v_{\bar{p}}. \tag{4.57}
\end{aligned}$$

The Clebsch-Gordon coefficients for weak Λp form factors are

$$d^{\Lambda p} = -\frac{1}{\sqrt{6}}, \quad f^{\Lambda p} = -\frac{3}{\sqrt{6}}. \tag{4.58}$$

Hence,

$$f_1^{\Lambda p}(t) = -\sqrt{\frac{3}{2}} F_1^p(t), \quad f_2^{\Lambda p}(t) = -\sqrt{\frac{3}{2}} F_2^p(t). \tag{4.59}$$

In the large t regime, the dominated axial form factor is [38]

$$g_1^{\Lambda p}(t) \rightarrow -\sqrt{\frac{3}{2}} G_M^p(t). \tag{4.60}$$

As the $\bar{B}^0 \rightarrow n \bar{p} \pi^+(\rho^+)$ decays, we consider two distinct empirical fits for the proton magnetic form factors denoted by CHT and BKLH. Using the same running quark masses as before we show the results of branching ratios in Table IV with and without the contributions from the axial form factor $g_1^{\Lambda p}$. When including the contribution from axial form factors we shall assume the validity of the relation (4.60) for all the range of t . We see that the predictions are quite sensitive to the baryonic form factors $f_i^{\Lambda p}$ and $g_i^{\Lambda p}$. It is evident from Table IV that the factorizable contributions to $\bar{B}^0 \rightarrow \Lambda \bar{p} \pi^+(\rho^+)$ are generally smaller than 1×10^{-6} , while the current limit is 1.3×10^{-5} [32]. Thus far we have neglected the nonfactorizable contributions from Fig. 2(e). The corresponding pole diagrams involve Σ_b^+ and Σ^+ poles. Unfortunately, it is not easy to evaluate the nonfactorizable weak matrix elements. It is conceivable that the total decay rate will be enhanced by a factor of 2. At any rate, we conclude that the branching ratios of $\bar{B}^0 \rightarrow \Lambda \bar{p} \pi^+$ are at most on the verge of 10^{-6} .

In Sec. IV.C below we shall explain why this penguin-dominated decay does not have a large rate. In contrast, the radiative baryonic decay $B^- \rightarrow \Lambda \bar{p} \gamma$ is likely to have an appreciable decay rate for two reasons. First, the main pole diagram for this radiative decay comes from the strong process $B^- \rightarrow \Lambda_b \bar{p}$ followed by the weak radiative transition $\Lambda_b \rightarrow \Lambda \gamma$. Since the latter is induced by the electromagnetic penguin mechanism $b \rightarrow s \gamma$, it has a magnitude of order 1×10^{-5} [55]. Second, the coupling of the Λ_b with the B meson and the nucleon is large. Our study indicates that $\mathcal{B}(B^- \rightarrow \Lambda \bar{p} \gamma) \approx (1 \sim 5) \times 10^{-6}$ [56]. Therefore, experimentally it would be quite interesting to measure the radiative baryonic B state $\Lambda \bar{p} \gamma$ and compare with $\Lambda \bar{p} \pi^+(\rho^+)$.

TABLE IV. Same as Table III except for $\bar{B}^0 \rightarrow \Lambda \bar{p} \pi^+(\rho^+)$. The axial form factor $g_1^{\Lambda p}(t)$ is taken to be the asymptotic form given by Eq. (4.60).

	G_M^p (CHT)		G_M^p (BKLH)	
	MS	BSW	MS	BSW
$\bar{B}^0 \rightarrow \Lambda \bar{p} \pi^+$	2.2×10^{-7}	3.4×10^{-7}	8.0×10^{-8}	1.2×10^{-7}
	2.9×10^{-7}	4.3×10^{-7}	8.5×10^{-8}	1.3×10^{-7}
$\bar{B}^0 \rightarrow \Lambda \bar{p} \rho^+$	2.3×10^{-7}	3.3×10^{-7}	6.6×10^{-8}	9.2×10^{-8}
	4.8×10^{-7}	6.4×10^{-7}	8.5×10^{-8}	1.2×10^{-7}

3. $\bar{B}^0 \rightarrow \Sigma^0 \bar{p} \pi^+(\rho^+)$ and $\bar{B}^0 \rightarrow \Sigma^- \bar{n} \pi^+(\rho^+)$

There are several other interesting penguin-dominated modes as listed in (4.3), for example $\bar{B}^0 \rightarrow \{\Sigma^0 \bar{p}, \Sigma^- \bar{n}, \Xi^- \bar{\Lambda}, \Xi^- \bar{\Sigma}^0\} \pi^+(\rho^+)$. The calculations are very similar to that of $\bar{B}^0 \rightarrow \Lambda \bar{p} \pi^+$. The relevant Clebsch-Gordon coefficients for weak form factors are

$$\begin{aligned} d^{\Sigma^0 p} &= \frac{1}{\sqrt{2}}, & f^{\Sigma^0 p} &= -\frac{1}{\sqrt{2}}, & d^{\Sigma^- n} &= 1, & f^{\Sigma^- n} &= -1, \\ d^{\Xi^- \Lambda} &= -\frac{1}{\sqrt{6}}, & f^{\Xi^- \Lambda} &= \frac{3}{\sqrt{6}}, & d^{\Xi^- \Sigma^0} &= \frac{1}{\sqrt{2}}, & f^{\Xi^- \Sigma^0} &= \frac{1}{\sqrt{2}}. \end{aligned} \quad (4.61)$$

Hence,

$$\begin{aligned} f_{1,2}^{\Sigma^0 p} &= -\frac{1}{\sqrt{2}}(F_{1,2}^p + 2F_{1,2}^n), & f_{1,2}^{\Sigma^- n} &= -(F_{1,2}^p + 2F_{1,2}^n), \\ f_{1,2}^{\Xi^- \Lambda} &= \frac{3}{\sqrt{6}}(F_{1,2}^p + F_{1,2}^n), & f_{1,2}^{\Xi^- \Sigma^0} &= \frac{1}{\sqrt{2}}(F_{1,2}^p - F_{1,2}^n), \end{aligned} \quad (4.62)$$

The dominated axial form factors in the large t regime are

$$g_1^{\Sigma^0 p}(t) \rightarrow \frac{1}{3\sqrt{2}}(G_M^p + 6G_M^n), \quad g_1^{\Sigma^- n}(t) \rightarrow \frac{1}{3}(G_M^p + 6G_M^n). \quad (4.63)$$

Obviously, $A(\bar{B}^0 \rightarrow \Sigma^- \bar{n} \pi^+(\rho^+)) = \sqrt{2}A(\bar{B}^0 \rightarrow \Sigma^0 \bar{p} \pi^+(\rho^+))$.

It turns out that the branching ratios of $\bar{B}^0 \rightarrow \Xi^- \bar{\Lambda}(\bar{\Sigma}^0) \pi^+$, being of order 5×10^{-8} , are even smaller than the $\Lambda \bar{p} \pi^+$ final state. Therefore, only the results for $\Sigma \bar{N} \pi^+(\rho^+)$ are shown in Table V. We see that (i) branching ratios of $\Sigma^- \bar{n} \pi^+(\rho^+)$ lie in the ranges of $(1.0 \sim 2.2) \times 10^{-6}$ and $(0.6 \sim 1.6) \times 10^{-6}$, respectively. Thus the ratio of ρ^+/π^+ is not greater than unity, contrary to the case of $\bar{B}^0 \rightarrow p \bar{n} \pi^-(\rho^-)$. (ii) The decay rate of $\Sigma^- \bar{n} \pi^+(\rho^+)$ is two times as large as that of $\Sigma^0 \bar{p} \pi^+(\rho^+)$, but the latter will be more easy to detect experimentally.

4. $\bar{B}^0 \rightarrow \eta' \Lambda \bar{p}$

TABLE V. Same as Table III except for $\bar{B}^0 \rightarrow \Sigma \bar{N} \pi^+(\rho^+)$. The axial form factor $g_1(t)$ is taken to be the asymptotic form given by Eq. (4.63).

	G_M^p (CHT)		G_M^p (BKLH)	
	MS	BSW	MS	BSW
$\bar{B}^0 \rightarrow \Sigma^0 \bar{p} \pi^+$	1.0×10^{-6}	1.6×10^{-6}	1.4×10^{-6}	2.0×10^{-6}
	1.1×10^{-6}	1.8×10^{-6}	1.2×10^{-6}	2.2×10^{-6}
$\rightarrow \Sigma^0 \bar{p} \rho^+$	6.9×10^{-7}	6.0×10^{-7}	1.0×10^{-6}	1.0×10^{-6}
	1.2×10^{-6}	1.0×10^{-6}	1.6×10^{-6}	1.5×10^{-6}
$\rightarrow \Sigma^- \bar{n} \pi^+$	1.9×10^{-6}	3.3×10^{-6}	2.4×10^{-6}	4.1×10^{-6}
	2.2×10^{-6}	3.7×10^{-6}	2.7×10^{-6}	4.5×10^{-6}
$\rightarrow \Sigma^- \bar{n} \rho^+$	1.4×10^{-6}	1.2×10^{-6}	2.0×10^{-6}	2.0×10^{-6}
	2.4×10^{-6}	2.1×10^{-6}	3.2×10^{-6}	3.0×10^{-6}

It has been argued in [17] that $\bar{B} \rightarrow \eta' \mathcal{B}_s \bar{B}$ could be the most promising charmless baryonic modes; they may be comparable to the $\eta' K$ and a crude estimate yields $\Gamma(\bar{B}^0 \rightarrow \eta' \Lambda \bar{p}) \approx 0.3 \Gamma(B \rightarrow \eta' K)$. Of course, the study of $\eta' \Lambda \bar{p}$ is much more complicated than $\eta' K$: The factorizable amplitudes for the former involves several 3-body matrix elements that are difficult to evaluate. Another complication is that what is the role played by the gluon anomaly is still controversial and not clear even for $\eta' K$ modes, not mentioning the three-body one, $\eta' \mathcal{B}_s \bar{B}$. A detailed study of $\bar{B} \rightarrow \eta' \Lambda \bar{p}$ will be presented elsewhere.

C. When do we have $\Gamma(\bar{B} \rightarrow \mathcal{B}_1 \bar{\mathcal{B}}_2 M) > \Gamma(\bar{B} \rightarrow \mathcal{B}_1 \bar{\mathcal{B}}_2)$?

As discussed in the beginning of this section, the question of why some of three-body baryonic B decays in which baryon-antibaryon pair production is accompanied by a meson have larger rates than their two-body counterparts can be qualitatively understood in terms of the Dalitz plot analysis which indicates that, for example, the diquark ud has a very large invariant mass due to the $V - A$ nature of the $b \rightarrow ud\bar{u}$ process [34,35]. If the ud forms a nucleon, then it will tend to form a highly excited baryon and will be seen as $Nn\pi (n \geq 1)$. This explains why $N\bar{N}$ final states have small rates, why $p\bar{\Delta}$ and $\Sigma\bar{\Delta}$ states are leading tree-dominated and penguin-dominated two-body baryonic B decay modes, and why the three-body mode $N\bar{N}\pi(\rho)$ is favored over the two-body one. From the calculations in Sections III and IV, we can give a more quantitative statement.

The experimental fact that the penguin-dominated decay $B^- \rightarrow p\bar{p}K^-$ has a magnitude larger than the two-body counterpart $\bar{B}^0 \rightarrow p\bar{p}$ can be easily explained in the language of the pole model. The intermediate pole states are $\Lambda_b^{(*)}$ and $\Sigma_b^{(*)}$ for the above-mentioned three-body final state and $\Sigma_b^{(*)}$ for the two-body one. First, the Σ_b propagator in the pole

amplitude for the latter is of order $1/(m_b^2 - m_B^2)$, while the invariant mass of the (pK^-) system can be large enough in the former decay so that the propagator in the pole diagram is no longer subject to the same $1/m_b^2$ suppression. Second, Λ_b (and the anti-triplet bottom baryon Ξ_b) has a much larger coupling to the B meson and the light octet baryon \mathcal{B} than Σ_b [see Eq. (3.23)]. These two effects will overcome the three-body phase space suppression to render the three-body mode dominant. The other examples in this category are $\Gamma(\bar{B}^0 \rightarrow p\bar{n}\pi^-) > \Gamma(B^- \rightarrow n\bar{p})$ as shown before and $\Gamma(B^- \rightarrow \Lambda_c\bar{p}\pi^-) > \Gamma(\bar{B}^0 \rightarrow \Lambda_c\bar{p})$ as discussed in [21]. We have shown before that $\Gamma(\bar{B}^0 \rightarrow n\bar{p}\pi^+) > \Gamma(B^- \rightarrow n\bar{p})$ even though the pole diagram for the former does not have a Λ_b pole. This can be comprehended from the observation that the former is dominated by the external W -emission contribution governed by the parameter a_1 , while the latter proceeds via the internal W emission process. If the aforementioned conditions are not satisfied, then the three-body mode will not necessarily have larger branching ratios than the corresponding two-body ones. For example, the penguin-dominated decays $\bar{B}^0 \rightarrow p\bar{p}\bar{K}^0$, $n\bar{n}\bar{K}^0$ proceed through the $\Sigma_b^{(*)}$ pole only and hence their rates are suppressed. The penguin-dominated decays $\bar{B}^0 \rightarrow \Lambda\bar{p}\pi^+(\rho^+)$ are also suppressed relative to $p\bar{p}K^{(*)}$ modes due to the lack of Λ_b poles. Indeed, we found their magnitude does not exceed 1×10^{-6} .

V. DISCUSSIONS AND CONCLUSIONS

We have presented a systematical study of two-body and three-body charmless baryonic B decays. We first draw some conclusions from our analysis and then proceed to discuss the sources of theoretical uncertainties during the course of calculation.

1. The two-body baryonic B decay $B \rightarrow \mathcal{B}_1\bar{\mathcal{B}}_2$ receives main contributions from the internal W -emission diagram for tree-dominated modes and the penguin diagram for penguin-dominated processes. We evaluate the corresponding pole diagrams to calculate the nonfactorizable contributions. The parity-conserving baryon matrix elements are estimated using the MIT bag model. We found that the bag-model estimate of baryon matrix elements are about three times as small as the previous calculation based on the harmonic oscillator model. The predicted branching ratios for two-body modes are in general very small, typically less than 10^{-6} , except for the case with a Δ resonance in the final state. Physically, this is because the diquark system in b decay has a very large invariant mass and hence it tends to form a highly excited baryon state such as the Δ and will be seen as $Nn\pi (n \geq 1)$, for example. This also explains the non-observation of the $N\bar{N}$ final states. We found that the tree-dominated decay $B^- \rightarrow p\bar{\Delta}^{--}$ can be of order 10^{-6} due to the large coupling of the Δ with the B meson and the octet baryon. This charmless two-body baryonic mode should be readily accessible by B factories BaBar and Belle.

2. Owing to large theoretical uncertainties with parity-violating matrix elements, we focus only on the parity-conserving contributions for two-body final states. Nevertheless, $B^- \rightarrow n\bar{p}$, $\bar{B} \rightarrow N\bar{\Delta}$ and $\Sigma\bar{\Delta}$ are purely parity-conserving, whereas $\bar{B}^0 \rightarrow \Lambda\bar{\Lambda}$ is purely parity-violating, provided that the quark pair is created from the vacuum with vacuum quantum numbers (3P_0 model). These features can be tested by measuring decay asymmetries or longitudinal polarizations.
3. Although three-body modes in general receive factorizable contributions, not all of them are calculable in practice due mainly to the lack of information for three-body hadronic matrix elements. Therefore, in many cases we still have to rely on the pole approximation to evaluate the factorizable amplitudes.
4. For three-body modes we focus on octet baryon final states. The tree-dominated modes $\bar{B}^0 \rightarrow n\bar{p}\pi^+(\rho^+)$ have a branching ratio of order $(1 \sim 4) \times 10^{-6}$ for the π^+ production and $(3 \sim 5) \times 10^{-6}$ for the ρ^+ production. Moreover, $\mathcal{B}(\bar{B}^0 \rightarrow p\bar{n}\pi^-) \sim 3 \times 10^{-6}$ and $\mathcal{B}(\bar{B}^0 \rightarrow p\bar{n}\rho^-) \sim 8 \times 10^{-6}$ are predicted. There are some theoretical uncertainties for the prediction of $B^- \rightarrow p\bar{p}\pi^-$ and it is conjectured to have a branching ratio of order 10^{-6} .
5. Assuming a monopole q^2 dependence for heavy-to-light baryon form factors, we predict that $\mathcal{B}(B^- \rightarrow p\bar{p}K^-) \sim 4 \times 10^{-6}$ and the other penguin-dominated decays $B^- \rightarrow p\bar{p}K^{*-}$, $\bar{B}^0 \rightarrow p\bar{n}K^-$ and $\bar{B}^0 \rightarrow p\bar{n}K^{*-}$ all have the branching ratio of order 2×10^{-6} and their $N\bar{N}$ mass spectra peak at low mass. The first one is consistent with the recent measurement of $B^- \rightarrow p\bar{p}K^-$ by Belle. Therefore, several $B \rightarrow N\bar{N}K^{(*)}$ decays should be easily seen by B factories at the present level of sensitivity. The study of the differential decay rate of $B^- \rightarrow p\bar{p}K^-$ clearly indicates a threshold baryon pair production and a fast recoil meson accompanied by a low mass baryon pair.
6. The predictions of tree-dominated decays $\bar{B} \rightarrow p\bar{p}/n\bar{p}$, $\bar{B} \rightarrow N\bar{\Delta}$ and penguin-dominated modes $\bar{B} \rightarrow \Sigma\bar{p}$, $\Sigma\bar{\Delta}$ in the QCD sum-rule approach and the diquark model are quite different from the present work. Measurements of the above-mentioned modes can differentiate between the different approaches.
7. The factorizable contributions to the penguin-dominated decays containing a strange baryon, e.g., $\bar{B}^0 \rightarrow \Sigma^0\bar{p}\pi^+(\rho^+)$, $\Sigma^-\bar{n}\pi^+(\rho^+)$, $\Lambda\bar{p}\pi^+(\rho^+)$, are calculable. While the $\Sigma\bar{N}\pi^+$ state has a sizable rate, of order $(1 - 3) \times 10^{-6}$, the branching ratios of $\bar{B}^0 \rightarrow \Lambda\bar{p}\pi^+(\rho^+)$ are in general smaller than 10^{-6} .
8. Some of charmless three-body final states have a larger rate than their two-body counterparts because (i) the propagator in the pole diagrams for the three-body final state is not suppressed by $1/m_b^2$, and (ii) in general the pole diagram of the former contains a Λ_b or Ξ_b intermediate state which has a large coupling to the B meson and the light baryon, for example $\Gamma(\bar{B}^0 \rightarrow p\bar{n}\pi^-) > \Gamma(B^- \rightarrow n\bar{p})$, $\Gamma(B^- \rightarrow p\bar{p}K^-) > \Gamma(\bar{B}^0 \rightarrow p\bar{p})$,

or (iii) some three-body baryonic decays are dominated by the factorizable external W -emission governed by the parameter a_1 , for example, $\Gamma(\overline{B}^0 \rightarrow n\bar{p}\pi^+) > \Gamma(B^- \rightarrow n\bar{p})$.

Needless to say, the calculation of baryonic B decays is rather complicated and very much involved and hence it suffers from several possible theoretical uncertainties. Though most of them have been discussed before, it is useful to make a short summary here: (i) Since it is very difficult to evaluate nonfactorizable and even some of factorizable amplitudes, we have relied on the pole approximation that, at the hadron level, these amplitudes are manifested as the pole diagrams with low-lying one-particle intermediate states. We use the bag model to evaluate the baryon matrix elements. Owing to the technical difficulties and the unreliability of the model for describing negative parity resonances, we limit ourselves to $\frac{1}{2}^+$ poles and hence consider only parity-conserving amplitudes. In the future we need a more sophisticated method to evaluate both PC and PV weak baryon matrix elements. Another important issue is that the intermediate pole state may be far from its mass shell and this will affect the applicability of the quark-model estimate of baryonic matrix elements. (ii) We have applied the 3P_0 quark-pair-creation model to estimate relative strong coupling strengths. This amounts to treating the strong $B\mathcal{B}_b\mathcal{B}$ coupling as point-like or assuming its relative magnitude not being affected by the momentum dependence. However, it is not clear to us how good this approximation is. In the future, it is important to have a solid pQCD analysis to understand this issue. (iii) Heavy-to-light baryon form factors are evaluated in the non-relativistic quark model at zero recoil. However, their q^2 dependence is basically unknown. We have resorted to the pole dominance approximation by assuming a simple monopole or dipole momentum dependence. The unknown momentum dependence for baryon form factors is one of the major theoretical uncertainties. (iv) We have applied SU(3) symmetry to relate the octet-octet baryonic vector form factors to the magnetic and electric form factors of the nucleon. Experimentally, one certainly needs measurements of nucleon (especially neutron) electromagnetic form factors for a large range of q^2 . Theoretically, it is important to know how important the SU(3) breaking effect is and how to treat the baryonic axial form factors. (v) The three-body decays usually proceed through several quark diagrams. To simplify the calculation and to catch the main physics, we have often focused only on the leading factorizable quark diagrams. It remains to investigate nonfactorizable contributions to see their relevance.

To conclude, we have pointed out several promising charmless two-body and three-body baryonic B decay modes which have branching ratios in the range of $10^{-5} \sim 10^{-6}$ and hence should be measurable by B factories.

ACKNOWLEDGMENTS

H.Y.C. wishes to thank C.N. Yang Institute for Theoretical Physics at SUNY Stony Brook for its hospitality. K.C.Y. would like to thank the Theory Group at the Institute of Physics, Academia Sinica, Taipei, Taiwan for its hospitality. This work was supported in part by the National Science Council of R.O.C. under Grant Nos. NSC90-2112-M-001-047 and NSC90-2112-M-033-004.

APPENDICES

A. BARYON WAVE FUNCTIONS

We list the spin-flavor wave functions of baryons relevant for our purposes:

$$\begin{aligned}
\Lambda_b^\uparrow &= \frac{1}{\sqrt{6}}[(bud - bdu)\chi_A + (12) + (13)], \\
\Xi_b^{0\uparrow} &= \frac{1}{\sqrt{6}}[(bus - bsu)\chi_A + (12) + (13)], \\
\Xi_b^{'0\uparrow} &= \frac{1}{\sqrt{6}}[(bus + bsu)\chi_s + (12) + (13)], \\
\Sigma_b^{+\uparrow} &= \frac{1}{\sqrt{3}}[buu\chi_s + (12) + (13)], \\
\Sigma_b^{0\uparrow} &= \frac{1}{\sqrt{6}}[(bud + bdu)\chi_s + (12) + (13)], \\
\Sigma_b^{-\uparrow} &= \frac{1}{\sqrt{3}}[bdd\chi_s + (12) + (13)], \\
\Sigma^{+\uparrow} &= \frac{1}{\sqrt{3}}[suu\chi_s + (12) + (13)], \\
\Sigma^{0\uparrow} &= \frac{1}{\sqrt{6}}[(sud + sdu)\chi_s + (12) + (13)], \\
\Sigma^{-\uparrow} &= \frac{1}{\sqrt{3}}[sdd\chi_s + (12) + (13)], \\
\Lambda^\uparrow &= \frac{1}{\sqrt{6}}[(sud - sdu)\chi_A + (12) + (13)], \\
p^\uparrow &= \frac{1}{\sqrt{3}}[duu\chi_s + (12) + (13)], \\
n^\uparrow &= \frac{1}{\sqrt{3}}[udd\chi_s + (12) + (13)], \\
\Delta^{++\uparrow} &= uuu\chi, \\
\Delta^{+\uparrow} &= \frac{1}{\sqrt{3}}[duu\chi + (12) + (13)], \\
\Delta^{0\uparrow} &= \frac{1}{\sqrt{3}}[udd\chi + (12) + (13)],
\end{aligned} \tag{A1}$$

where $abc\chi_s = (2a^\downarrow b^\uparrow c^\uparrow - a^\uparrow b^\uparrow c^\downarrow - a^\uparrow b^\downarrow c^\uparrow)/\sqrt{6}$, $abc\chi_A = (a^\uparrow b^\uparrow c^\downarrow - a^\uparrow b^\downarrow c^\uparrow)/\sqrt{2}$, $abc\chi = (a^\downarrow b^\uparrow c^\uparrow + a^\uparrow b^\uparrow c^\downarrow + a^\uparrow b^\downarrow c^\uparrow)/\sqrt{3}$, and (ij) means permutation for the quark in place i with the quark in place j . The spin-flavor wave function of the Δ is expressed for $S_z = \frac{1}{2}$. The relative sign of baryon-pseudoscalar couplings is then fixed.

B. BARYON MATRIX ELEMENTS IN THE BAG MODEL

Some of the details for evaluating the baryon matrix elements in the MIT bag model are already shown in [28,21]. Here we add the result for the matrix element of $(V - A)(V + A)$ current. Consider the four-quark operator $O = (\bar{q}_a q_b)_{V-A} (\bar{q}_c q_d)_{V-A}$. It can be written as $O(x) = 6(\bar{q}_a q_b)_{V-A}^1 (\bar{q}_c q_d)_{V-A}^2$ where the superscript i on the r.h.s. of O indicates that the quark operator acts only on the i th quark in the baryon wave function. Applying the relations

$$\begin{aligned}\langle q' | V_0 | q \rangle &= u' u + v' v, \\ \langle q' | A_0 | q \rangle &= -i(u' v - v' u) \vec{\sigma} \cdot \hat{r}, \\ \langle q' | \vec{V} | q \rangle &= -(u' v + v' u) \vec{\sigma} \times \hat{r} - i(u' v - v' u) \hat{r}, \\ \langle q' | \vec{A} | q \rangle &= (u' u - v' v) \vec{\sigma} + 2v' v \hat{r} \vec{\sigma} \cdot \hat{r},\end{aligned}\tag{B1}$$

leads to the PC matrix elements

$$\begin{aligned}\int r^2 dr \langle q_1^a q_2^c | (\bar{q}_a q_b)_{V-A}^1 (\bar{q}_c q_d)_{V-A}^2 | q_1^b q_2^d \rangle_{\text{PC}} &= X_1 + X_2 + (X_1 - X_2) \vec{\sigma}_1 \cdot \vec{\sigma}_2 - 2X_1 (\vec{\sigma}_1 \cdot \hat{r}) (\vec{\sigma}_2 \cdot \hat{r}) \\ &= X_1 + X_2 + \frac{1}{3} (X_1 - 3X_2) \vec{\sigma}_1 \cdot \vec{\sigma}_2,\end{aligned}\tag{B2}$$

for $(V - A)(V - A)$ current, where we have used the relation

$$\int d\Omega \hat{r}_i \hat{r}_j = \frac{\delta_{ij}}{3} \int d\Omega,\tag{B3}$$

and X_1 , X_2 are the bag integrals

$$\begin{aligned}X_1 &= \int_0^R r^2 dr [u_a(r)v_b(r) - v_a(r)u_b(r)][u_c(r)v_d(r) - v_c(r)u_d(r)], \\ X_2 &= \int_0^R r^2 dr [u_a(r)u_b(r) + v_a(r)v_b(r)][u_c(r)u_d(r) + v_c(r)v_d(r)],\end{aligned}\tag{B4}$$

with $u_q(r)$ and $v_q(r)$ being the large and small components, respectively, of the $1S_{1/2}$ quark wave function (see [28,21] for detail). Likewise, for $(V - A)(V + A)$ current we obtain

$$\int r^2 dr \langle q_1^a q_2^c | (\bar{q}_a q_b)_{V-A}^1 (\bar{q}_c q_d)_{V+A}^2 | q_1^b q_2^d \rangle_{\text{PC}} = (X_1 + X_2) + \frac{1}{3} [X_1 + X_2 - 2(X'_1 - X'_2)] \vec{\sigma}_1 \cdot \vec{\sigma}_2,\tag{B5}$$

with

$$\begin{aligned}X'_1 &= \int_0^R r^2 dr [u_a(r)v_b(r) + v_a(r)u_b(r)][u_c(r)v_d(r) + v_c(r)u_d(r)], \\ X'_2 &= \int_0^R r^2 dr [u_a(r)u_b(r) - v_a(r)v_b(r)][u_c(r)u_d(r) - v_c(r)v_d(r)].\end{aligned}\tag{B6}$$

For numerical estimates of the bag integrals, we shall use the bag parameters

$$\begin{aligned}m_u = m_d &= 0, & m_s &= 0.279 \text{ GeV}, & m_c &= 1.551 \text{ GeV}, & m_b &= 5.0 \text{ GeV}, \\ x_u = 2.043, & x_s = 2.488, & x_c = 2.948, & x_b = 3.079, & R &= 5.0 \text{ GeV}^{-1}.\end{aligned}\tag{B7}$$

REFERENCES

- [1] ARGUS Collaboration, H. Albrecht, *Phys. Lett.* **B209**, 119 (1988).
- [2] N.G. Deshpande, J. Trampetic, and A. Soni, *Mod. Phys. Lett.* **A3**, 749 (1988).
- [3] N. Paver and Riazuddin, *Phys. Lett.* **B201**, 279 (1988).
- [4] M. Gronau and J.L. Rosner, *Phys. Rev.* **D37**, 688 (1988); G. Eilam, M. Gronau, and J.L. Rosner, *Phys. Rev.* **D39**, 819 (1989).
- [5] J.G. Körner, *Z. Phys.* **C43**, 165 (1989).
- [6] A.V. Dobrovolskaya and A.B. Kaidalov, *JETP Lett.* **49**, 25 (1989).
- [7] V. Chernyak and I. Zhitnitsky, *Nucl. Phys.* **B345**, 137 (1990).
- [8] X.G. He, B.H.J. McKellar, and D.d. Wu, *Phys. Rev.* **D41**, 2141 (1990).
- [9] G. Lu, X. Xue, and J. Liu, *Phys. Lett.* **B259**, 169 (1991).
- [10] M. Jarfi *et al.*, *Phys. Rev.* **D43**, 1599 (1991); *Phys. Lett.* **B237**, 513 (1990).
- [11] P. Ball and H.G. Dosch, *Z. Phys.* **C51**, 445 (1991).
- [12] S.M. Sheikholeslami and M.P. Khanna, *Phys. Rev.* **D44**, 770 (1991); S.M. Sheikholeslami, G.K. Sindana, and M.P. Khanna, *Int. J. Mod. Phys.* **A7**, 1111 (1992).
- [13] G. Kaur and M.P. Khanna, *Phys. Rev.* **D46**, 466 (1992).
- [14] CLEO Collaboration, T.E. Coan *et al.*, *Phys. Rev.* **D59**, 111101 (1999).
- [15] Belle Collaboration, K. Abe *et al.*, hep-ex/0203027.
- [16] I. Dunietz, *Phys. Rev.* **D58**, 094010 (1998).
- [17] W.S. Hou and A. Soni, *Phys. Rev. Lett.* **86**, 4247 (2001).
- [18] C.K. Chua, W.S. Hou, and S.Y. Tsai, *Phys. Lett.* **B528**, 233 (2002).
- [19] CLEO Collaboration, S. Anderson *et al.*, *Phys. Rev. Lett.* **86**, 2732 (2001).
- [20] C.K. Chua, W.S. Hou, and S.Y. Tsai, *Phys. Rev.* **D65**, 034003 (2002).
- [21] H.Y. Cheng and K.C. Yang, *Phys. Rev.* **D65**, 054028 (2002); *ibid* **D65**, Erratum, 099901 (2002).
- [22] CLEO Collaboration, X. Fu *et al.*, *Phys. Rev. Lett.* **79**, 3125 (1997).
- [23] Belle Collaboration, K. Abe *et al.*, *Phys. Rev. Lett.* **88**, 181803 (2002); talk presented by H. Yamamoto at The Fifth KEK Topical Conference, Nov. 20-22, 2001.

- [24] G. Buchalla, A.J. Buras, and M.E. Lautenbacher, *Rev. Mod. Phys.* **68**, 1125 (1996).
- [25] Y.H. Chen, H.Y. Cheng, B. Tseng, and K.C. Yang, *Phys. Rev.* **D60**, 094014 (1999); A. Ali, G. Kramer, and C.D. Lü, *Phys. Rev.* **D58**, 094009 (1998).
- [26] H.Y. Cheng and K.C. Yang, *Phys. Rev.* **D62**, 054029 (2000).
- [27] L. Wolfenstein, *Phys. Rev. Lett.* **51**, 1945 (1983).
- [28] H.Y. Cheng and B. Tseng, *Phys. Rev.* **D46**, 1042 (1992); **55**, 1697(E) (1997).
- [29] H.Y. Cheng and B. Tseng, *Phys. Rev.* **D48**, 4188 (1993).
- [30] A. Chodos, R.L. Jaffe, K. Johnson, and C.B. Thorn, *Phys. Rev.* **D10**, 2599 (1974); T. DeGrand, R.L. Jaffe, K. Johnson, and J. Kisis, *ibid* **12**, 2060 (1975).
- [31] A. Le Yaouanc, L. Oliver, O. Péne, and J.-C. Raynal, *Hadron Transitions in the Quark Model* (Gordon and Breach Science Publishers, 1988).
- [32] Particle Data Group, D.E. Groom *et al.*, *Eur. Phys. J.* **C15**, 1 (2000).
- [33] C.H. Chang and W.S. Hou, hep-ph/0112219.
- [34] G. Buchalla, I. Dunietz, and H. Yamamoto, *Phys. Lett.* **B364**, 188 (1995).
- [35] I. Dunietz, hep-ph/9606247.
- [36] D. Bailin, *Weak Interactions* (Sussex University Press, London, 1982).
- [37] E.J. Brash, A. Kozlov, Sh. Li, and G.M. Huber, hep-ex/0111038.
- [38] S.J. Brodsky, G.P. Lepage, and S.A.A. Zaidi, *Phys. Rev.* **D23**, 1152 (1981).
- [39] M. Wirbel, B. Stech, and M. Bauer, *Z. Phys.* **C29**, 637 (1985); M. Bauer, B. Stech, and M. Wirbel, *Z. Phys.* **C34**, 103 (1987).
- [40] P. Ball and V.M. Braun, *Phys. Rev.* **D58**, 094016 (1998); P. Ball, *J. High Energy Phys.* **9809**, 005 (1998) [hep-ph/9802394].
- [41] D. Melikhov and B. Stech, *Phys. Rev.* **D62**, 014006 (2001).
- [42] Q.P. Xu, *Phys. Lett.* **B306**, 363 (1993); M. Neubert and V. Rieckert, *Nucl. Phys.* **B382**, 97 (1992).
- [43] H.Y. Cheng and B. Tseng, *Phys. Rev.* **D53**, 1457 (1996).
- [44] H.Y. Cheng, *Phys. Rev.* **D56**, 2799 (1997).
- [45] E. Jenkins, A. Manohar, and M.B. Wise, *Nucl. Phys.* **B396**, 38 (1993).
- [46] M. Sadzikowski and K. Zalewski, *Z. Phys.* **C59**, 677 (1993).

- [47] X.-H. Guo and P. Kroll, *Z. Phys. C***59**, 567 (1993); X.-H. Guo and T. Muta, *Mod. Phys. Lett. A***11**, 1523 (1996); *Phys. Rev. D***54**, 4629 (1996).
- [48] Y.B. Dai, C.S. Huang, M.Q. Huang, and C. Liu, *Phys. Lett. B***387**, 379 (1996).
- [49] M.A. Ivanov, V.E. Lyubovitskij, J.G. Körner, and P. Kroll, *Phys. Rev. D***56**, 348 (1997).
- [50] M.A. Ivanov, J.G. Körner, V.E. Lyubovitskij, and A.G. Rusetsky, *Phys. Rev. D***59**, 074016 (1999).
- [51] CLEO Collaboration, D. Cronin-Hennessy *et al.*, *Phys. Rev. Lett.* **85**, 515 (2000); Belle Collaboration, K. Abe *et al.*, *Phys. Rev. Lett.* **87**, 101801 (2001); BaBar Collaboration, B. Aubert *et al.*, *Phys. Rev. Lett.* **87**, 151802 (2001).
- [52] H.Y. Cheng, *Phys. Rev. D***65**, 094012 (2002).
- [53] Belle Collaboration, K. Abe *et al.*, *Phys. Rev. Lett.* **88**, 052002 (2002); CLEO Collaboration, T.E. Coan *et al.*, *Phys. Rev. Lett.* **88**, 062001 (2002).
- [54] H.Y. Cheng and K.C. Yang, *Phys. Rev. D***59**, 092004 (1999).
- [55] H.Y. Cheng, C.Y. Cheung, G.L. Lin, Y.C. Lin, T.M. Yan and H.L. Yu, *Phys. Rev. D***51**, 1199 (1995).
- [56] H.Y. Cheng and K.C. Yang, *Phys. Lett. B***533**, 271 (2002).